research articles Journal of proteome research

Stress Responses and Conditioning Effects in Mesothelial Cells Exposed to Peritoneal Dialysis Fluid

Klaus Kratochwill,[†] Michael Lechner,[‡] Christian Siehs,[§] Hans C. Lederhuber,[†] Pavel Rehulka,[||] Michaela Endemann,[†] David C. Kasper,[†] Kurt R. Herkner,[†] Bernd Mayer,[§] Andreas Rizzi,[‡] and Christoph Aufricht*,[†]

Department of Pediatrics and Adolescent Medicine, Medical University of Vienna, Austria, Institute of Analytical Chemistry and Food Chemistry, University of Vienna, Austria, Emergentec Biodevelopment GmbH, Vienna, Austria, and Institute of Analytical Chemistry, Academy of Sciences of the Czech Republic, Brno, Czech Republic

Received October 29, 2008

Renal replacement therapy by peritoneal dialysis is frequently complicated by technical failure. Peritoneal dialysis fluids (PDF) cause injury to the peritoneal mesothelial cell layer due to their cytotoxicity. As only isolated elements of the involved cellular processes have been studied before, we aimed at a global assessment of the mesothelial stress response to PDF. Following single or repeated exposure to PDF or control medium, proteomics and bioinformatics techniques were combined to study effects in mesothelial cells (MeT-5A). Protein expression was assessed by two-dimensional gel electrophoresis, and significantly altered spots were identified by MALDI-TOF MS and MS^2 techniques. The lists of experimentally derived candidate proteins were expanded by a next neighbor approach and analyzed for significantly enriched biological processes. To address the problem of an unknown portion of false positive spots in 2DGE, only proteins showing significant *p*-values on both levels were further interpreted. Single PDF exposure resulted in reduction of biological processes in favor of reparative responses, including protein metabolism, modification and folding, with chaperones as a major subgroup. The observed biological processes triggered by this acute PDF exposure mainly contained functionally interwoven multitasking proteins contributing as well to cytoskeletal reorganization and defense mechanisms. Repeated PDF exposure resulted in attenuated protein regulation, reflecting inhibition of stress responses by high levels of preinduced chaperones. The identified proteins were less attributable to acute cellular injury but rather to specialized functions with a reduced number of involved multitasking proteins. This finding agrees well with the concept of conditioning effects and cytoprotection. In conclusion, this study describes the reprogrammed proteome of mesothelial cells during recovery from PDF exposure and adaption to repetitive stress. A broad stress response with a number of highly overlapping processes and multitasking proteins shifts toward a more specific response of only few less overlapping processes.

Keywords: proteomics • heat shock proteins • pretreatment • bioinformatics analysis • protein interaction networks • 2D gel electrophoresis • pathway analysis

Introduction

Peritoneal dialysis (PD) is a safe and cost-effective mode of renal replacement therapy. With the use of the peritoneum as a semipermeable dialysis membrane, PD fluid (PDF) is repeatedly filled to and drained from the abdominal cavity. On the basis of its hypertonicity, PDF removes solutes and water from the uremic patient. However, prolonged PD treatment frequently leads to severe chronic damage to the integrity of the peritoneal membrane.[1] As it is virtually impossible to study the molecular effects of PDF exposure in the mesothelial cell monolayer lining the peritoneal cavity in the clinical setting, most researchers rely on *in vitro* cell culture models of PD for examining cytotoxicity of PDF.[2] In these models, exposure of human mesothelial cells to PDF results in cytotoxic insult, due to acidic pH, hyperosmolarity, and high concentration of lactate, glucose and its degradation products after heat sterilization.[3–10]

In previous studies, we have shown that the same cytotoxic insult that induces cellular injury also triggers cellular processes leading to repair and recovery in experimental PD.[11–13] Preinduction of this stress-response with a nonlethal dose results

* To whom correspondence should be addressed. Prof. Christoph Aufricht, Medizinische Unversität Wien/Univ. Klinik f. Kinder- and Jugenheilkunde, Währinger Gürtel 18-20, A-1090 Wien, Austria. Phone: +43 1 40400 2908; fax, +43 1 40400 3189; e-mail, christoph.aufricht@meduniwien.ac.at.
[†] Medical University of Vienna.
[‡] University of Vienna.
[§] Emergentec Biodevelopment GmbH.
[||] Academy of Sciences of the Czech Republic.

10.1021/pr800916s CCC: $40.75

Published on Web 02/20/2009

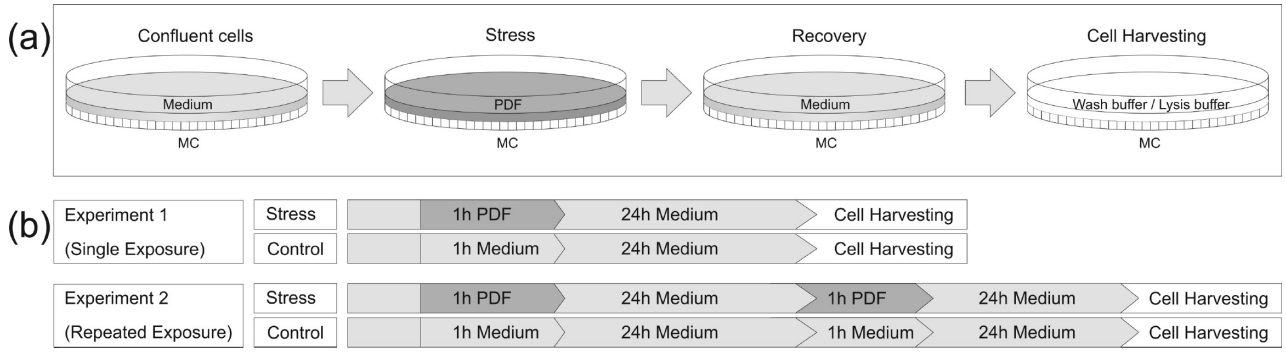

Figure 1. (a): Schematic representation of the experimental workflow. (b) Flowchart and time-course of the conducted stress experiments. Human mesothelial cells (MC) at confluence were either exposed to peritoneal dialysis fluid (PDF) or normal growth medium as the control for 1 h. Cells were then allowed to recover under normal growth medium for 24 h. For repeated exposure, the procedure was repeated once.

in survival of a subsequent usually lethal dose of the same or another injury.[14,15] Evidence for such conditioning effects has been found in pretreatment of human mesothelial cells by heat or by PDF.[16–18] This stress response involves numerous interdependently regulated molecular mechanisms, of which heat shock protein (HSP) expression constitutes an essential aspect of the cellular processes counteracting PDF toxicity.[15] However, in renal medulla derived cells, which are intrinsically resistant against hypertonicity and acidosis, it has been demonstrated that also several non-HSP proteins participate in the adaptation of these cells to an adverse environment.[19–23] In rat mesothelial cells, gene expression array studies furthermore elegantly showed that exposure to cytotoxic stimuli induced a heterogeneous expression pattern, simultaneously indicating apoptosis, mitotic arrest and the cellular stress response.[24] Finally, proteome analysis of permanently thermotolerant cell lines demonstrated differential expression of HSP and non-HSP proteins in thermoresistance.[25] Taken together, these data suggest that the cytoprotective cellular stress responses are complex, and that multiple effector proteins are relevant in cytoprotection. Up to now, no systematic data were available for the mesothelial system.

We applied proteome analysis as a particularly powerful tool to systematically study intracellular stress responses reflected by differential protein abundances. Two-dimensional gel electrophoresis (2DGE) still represents the means with the highest resolution in the proteomics field (in terms of simultaneously separated and detected intact proteins).[26] Gel-based proteomics, however, is known to involve characteristic limitations as membrane-bound proteins and low-abundance proteins such as transcription factors or members of signaling cascades are less likely detected,[27,28] although potentially highly relevant in the stress response. To overcome these experimental limitations, we utilized bioinformatic procedures for rationally expanding the list of identified candidate proteins.[29,30] This study describes the combination of proteomics and bioinformatics for analyzing the cellular stress response, thereby identifying effects of conditioning in mesothelial cells after single and repeated exposure to peritoneal dialysis fluid.

Materials and Methods

Standard chemicals were purchased from Sigma-Aldrich (St.Louis, MI) if not specified otherwise.

Cell Culture. Immortalized human mesothelial cells (MeT-5A, ATCC CRL-9444) were cultured in M199 medium (M4530, Sigma-Aldrich) supplemented with 50 U/mL penicillin, 50 μg/mL streptomycin, 0.4% HEPES and 10% FCS. Cultures were kept at 37 C in 5% CO_2 in 75 cm^2 tissue culture flasks (TPP-Techno Plastics Products AG, Trasadingen, Switzerland) for continuous growth and on 6 well plates (TPP) during PDF experiments. Cultures were passaged by regular trypsinization. Medium was changed every 2−3 days. Confluence was reached on average after 7−9 days. Control cultures were kept in regular culture media at 37 C and underwent the same "sham-procedures" of media changes. In the single exposure model, cultures were exposed to acidic lactate-based PDF (CAPD2, Fresenius, Bad Homburg, Germany) for 60 min and then allowed to recover in regular growth medium for 24 h. For the repeated injury model, the procedure was repeated by exposure to PDF for another 60 min and another recovery phase of 24 h using normal growth medium. After recovery, cells were washed with wash buffer (250 mM saccharose, 10 mM Tris/HCl, pH 7) 3 times, shock frozen using liquid nitrogen, and stored at −80 C for a maximum of 3 days. The stress experiments were conducted following the workflow shown in Figure 1. Three separate biological replicate experiments were conducted. Cell culturing for replicate 3 was again run in duplicate and one half of the samples was used for the repeated injury model.

Sample Preparation. Cells were lysed by incubation with 1 mL of lysis solution (7 M urea, 2 M thiourea, 4% 3-[(3-Cholamidopropyl)dimethylammonio]-1-propanesulfonate (CHAPS), 10 mM DTT, 1 mM EDTA, 0.5% Pharmalyte 3−10 (GE Healthcare, Uppsala, Sweden), and 1 tablet of Complete Protease Inhibitor (Roche, Basel, Switzerland) per 100 mL) per 3×10^7 cells for 45 min at 25 C. The resulting lysates were centrifuged for 45 min (14 000*g*, 10 C) and the supernatant was stored at −80 C until further processing. Samples were concentrated and desalted using a modified version of the precipitation protocol of Wessel and Flugge.[31] In brief, the samples were consecutively vortexed with 4 vol of methanol, 1 vol of chloroform and 3 vol of water. After centrifugation at 14 000*g* at 20 C, the upper aqueous layer was removed with a glass capillary. Four volumes of methanol was added and the samples were vortexed and centrifuged again (14 000*g*; 20 C). The supernatant was removed using a glass capillary and the precipitated proteins were left to air-dry for approximately 10 min. Subsequently, the proteins were reconstituted with solubilization buffer (7 M urea, 2 M thiourea, 4% CHAPS, 1 mM EDTA, 30 mM Tris/HCl, pH 8.5, and 1 tablet of Complete Mini Protease Inhibitor (Roche) per 100 mL) and left at 4−8 C overnight. Total protein concentration of the samples

was evaluated using the 2D-Qant kit (GE Healthcare) according to the manufacturer's manual.

Isoelectric Focusing and Second-Dimension SDS-PAGE. A total of 300 μg of total protein per IPG strip (Immobiline DryStrip pH 3−10, linear, 18 cm, GE Healthcare) was applied by rehydration loading using 6 technical replicates per sample. The volume of the rehydration mix was 340 μL with a final concentration of 5 M urea, 0.5% CHAPS, 0.5% Pharmalyte and 12 μL/mL of DeStreak reagent (GE Healthcare). During rehydration for 12−16 h, the IPG strips were sealed with DryStrip Cover Fluid (GE Healthcare). Isoelectric focusing (IEF) was accomplished on a Multiphor II (GE Healthcare) electrophoresis unit under DryStrip Cover Fluid at 20 C using the Immobiline DryStrip kit (GE Healthcare). Voltage was kept at 100 V for 3 h, then gradually increased to 3500 V in 2 h and kept constant for another 5.5 h. Current was limited to 50 μA/strip throughout the whole time. Focused strips were stored at −80 C until further use. The strips were consecutively incubated for 2 × 15 min in 10 mL equilibration buffer (6 M urea, 2% (w/v) SDS, 25% (w/v) glycerol, and 3.3% (v/v) 50 mM Tris/HCl buffer pH 8.8, stained with bromphenol blue for visibility of the front) first supplemented with 100 mg of DTT and then with 480 mg of 2-iodoacetamide. The second-dimension SDS-PAGE was carried out on Multiphor II electrophoresis units at 20 C according to the manufacturer's protocol using "Excelgel XL 12−14" ready cast gels and the appropriate cathodic and anodic buffer strips (all from GE Healthcare). The gel run was performed at 100 V, 25 mA, 30 W for 60 min in the first phase and 800 V, 40 mA, 50 W for 3 h in the second phase. After the first phase, the IPG strip was removed and the anodic buffer strip was moved forward to the position of the removed IPG strip. The run was stopped when the bromophenol blue stained front had reached the cathodic buffer strip.

Visualization of Proteins. All incubation steps were carried out on a horizontal rotary shaker at 80 rpm. Protein spots were fixed for 2 h with fixing solution (10% acetic acid, 40% ethanol). Gels were washed 3 times for 5 min with H_2O_{UHQ} and then incubated overnight in Coomassie Brilliant Blue (CBB) staining solution (8% (w/v) ammonium sulfate, 2% (v/v) ortho phosphoric acid (85%), 20% (v/v) methanol and 1% (v/v) CBB stock solution (2.5% (w/v) Coomassie Brilliant Blue G250 dissolved in H_2O_{UHQ})). The gels were then incubated in an aqueous solution containing 20% ammonium sulfate for 30 min and afterward 4 × 30 min in destaining solution (20% (v/v) methanol and 10% (v/v) glycerol (87%)). For prolonged storage, gels were sealed in plastic sheet protectors containing a few drops of H_2O_{UHQ} with a standard heat sealer and stored at 4−8 C in the dark.

Image Acquisition and Data Analysis. Gels were scanned on an Imagescanner II (GE Healthcare) using the Labscan 3.0 software package in transmission mode at 300 dpi, 16 bit gray scale without any manipulation of the raw data. Images were warped group-wise using Delta2D 3.6 software (Decodon GmbH, Greifswald, Germany). Spot patterns were detected on fused images (gained from all gels) using the average intensity algorithm and retransferred to the original images for 100% matching efficiency. Spot quantification was based on normalized relative spot volume (% volume) as exported from the statistics table of the Delta2D software.

Identification of Proteins by 1 and 2D-Western Analysis. For Western blot analysis, the gels were electroblotted onto a PVDF membrane immediately after the run by semidry transfer using the Novablot unit of the MultiPhor II electrophoresis system and the according transfer buffer (200 mM glycine, 25 mM Tris base, 0.1% SDS, and 20% methanol) following the manufacturer's manual. For 2D-Western analysis, the membrane was rehumidified with methanol, washed in TBST buffer (150 mM NaCl, 0.05% Tween 20, and 10 mM Tris/HCl at pH 7.4), and membranes were incubated with a solution of 0.2% Ponceau S (Sigma-Aldrich) in 3% trichloroacetic acid and 3% sulfosalicylic acid for 5 min. The membrane was washed extensively in water until the water was clear and highly abundant spots were well-defined. The membrane was scanned using an Imagescanner II (GE Healthcare) in reflective RGB mode (300 dpi). A number of highly abundant spots were marked as landmarks for later orientation on the membrane using a pencil. The membrane was destained completely by repeated washing in TBST and water, rehumidified with methanol and washed again in TBST buffer before proceeding to the blocking step. For 1D- and 2D-Western analysis, the membrane was blocked with 5% dry milk in TBST and then incubated with the primary antibody (HSPA1 (Hsp72) SPA-810, HSPB1 (Hsp27) SPA-800, SERPINH1 (Hsp47) SPA-470, PDIA3 (Erp57) SPA-725, P4HB (PDIA1) SPA-891, HSPD1 (Hsp60) SPA806, HSPA9 (Grp75) SPS-825, HSP90B1 (Hsp90) SPA-842 all from Stressgen/Assay Designs, Ann Arbor, MI; ANXA2 (Annexin II) ab54771, PPIA (Cyclophilin A) ab3563 all from Abcam, Camebridge, U.K.) for 16 h. After incubation with secondary, peroxidase-coupled antibodies (Polyclonal Rabbit Anti-Rat Ig/HRP P0450, Polyclonal Rabbit Anti-Mouse Ig/HRP P0260 both Dako Cytomation, Carpinteria, CA; Goat polyclonal to rabbit IgG - H&L (HRP) ab6721, Abcam), detection was accomplished by using enhanced chemiluminescence solution (Western Lightning reagent, Perkin-Elmer, Boston, MA) and a ChemiDoc XRS chemiluminescence detection system (Bio-Rad, Hercules, CA). Densitometric quantification of 1D bands was accomplished using the Bio-Rad QuantityOne software.

Identification of Proteins by Mass Spectrometry. Tryptic in-gel digestions of the excised protein spots were performed following the protocol of Shevchenko with slight modifications.[32] Gel plugs were excised with the aid of an Ettan Spot Picker (GE Healthcare) using the "export pick list" tool of the Delta2D software. Gel plugs were washed with water, water/acetonitrile (ACN) (Merck; Darmstadt, Germany) and 50 mM NH_4HCO_3 buffer/acetonitrile, altogether six times. Afterward, the sample was reduced by adding a 10 mM solution of DTT and incubating for 45 min at 56 C and alkylated by adding a 55 mM solution of iodoacetamide incubating over 30 min at 25 C in the dark (both were solutions in 50 mM NH_4HCO_3 buffer). The proteins were digested with a 12.5 ng/μL solution of trypsin (Sigma-Aldrich) in 50 mM NH_4HCO_3 buffer at 37 C overnight. The cleaved peptides were eluted from the gel pieces with 50 μL of 25 mM NH_4HCO_3 buffer (pH 8.5), 50 μL of 5% formic acid (Merck) and 50 μL 1:1 mixture of these solutions with acetonitrile. The pooled eluates were dried by vacuum centrifugation and the peptides were redissolved with 10 μL 0.1% TFA and sonicated briefly. The obtained solution was desalted by use of μ-C18 ZipTip columns (Millipore; Billerica, MA). First, the material was wetted with ACN and equilibrated with 0.1% TFA, then the sample was aspirated and expelled 10 times, followed by 5 washing steps with 0.1% TFA and finally eluted by α-cyano-4-hydroxycinnamic acid (Sigma-Aldrich) at a concentration of 10 mg/mL in ACN/0.1% TFA (3:2 v/v) onto the MALDI target (1 μL/spot, dried droplet method).

MALDI-TOF/TOF measurements in the positive ion mode were performed with the Applied Biosystems 4700 Proteomics

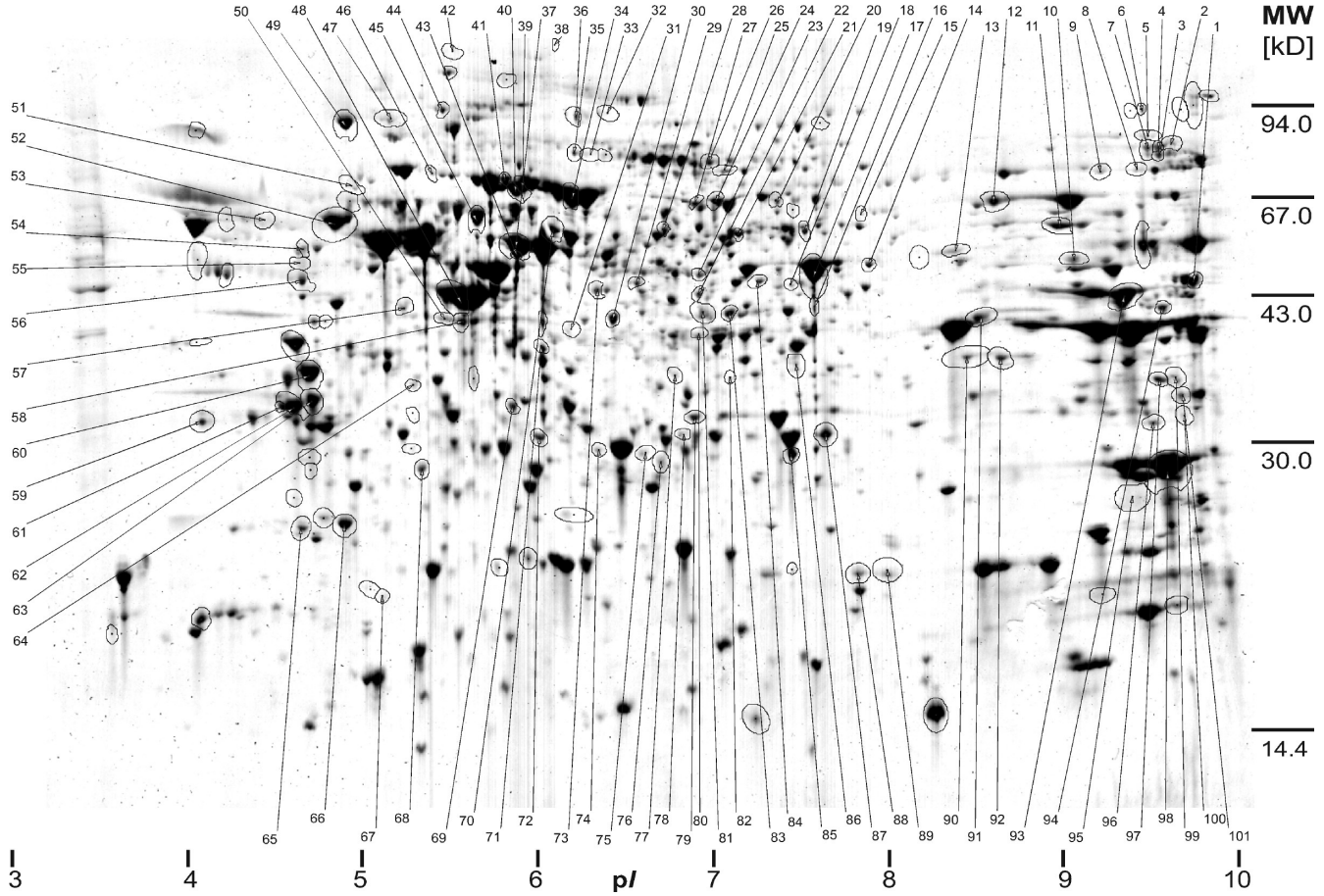

Figure 2. A representative Coomassie brilliant blue stained two-dimensional electrophoresis gel of the proteome of mesothelial cell (MeT-5A) lysates. Proteins were separated by isoelectric point (p*I*) in the first dimension and molecular weight (MW) in the second dimension. Spots with significantly altered abundance after single PDF exposure are indicated by circles. Identified proteins are marked with arrows and labeled by numbers referenced in Table 1.

Analyzer (Applied Biosystems, Framingham, MA). This TOF/TOF instrument is equipped with a Nd:YAG laser (355 nm) of 3−7 ns pulse and 200-Hz firing rate. Both MS and MS/MS spectra were acquired using dual-stage reflectron mirror. Accelerating voltages applied for MS and MS/MS measurements were 20 kV and 8 kV, respectively. In MS/MS mode, a collision energy of 1 kV was applied and nitrogen was used as a collision gas. MS spectra were calibrated externally using a mixture of 6 standard peptides in the m/z range from 904 to 3658 and MS/MS spectra were calibrated using angiotensin I ($m/z = 1296.6848$).

MS and MS/MS data were further processed using 4000 Series Explorer and GPS Explorer v. 3.6 (Applied Biosystems, Framingham, MA). Protein identification was carried out within the GPS Explorer program connected to the Mascot server (local installation, ver. 2.0.00) using the "Combined MS+MS/MS" database search method. Combined peak lists (from MS and MS/MS measurements) were extracted from the instrument spectra database using S/N limit 45 (MS spectra) and 30 (MS/MS spectra). Contaminant peaks (e.g., keratins, trypsin autolysis peaks, matrix clusters) were excluded within a 75 ppm tolerance from their theoretical values. The following parameters were used for the database searching: database, Swiss-Prot (ver. 54.6 from 4.12.2007); taxonomy, mammals; enzyme, trypsin; allowed missed cleavages, 1; fixed modifications, carbamidomethyl (C); variable modifications, none; peptide mass tolerance, 75 ppm; MS/MS tolerance, 250 mmu; peptide charge, (+1); monoisotopic masses; instrument, MALDI-TOF/TOF. Proteins were considered as identified when the confidence interval reported by GPS Explorer for the particular result from combined MS and MS/MS database search was higher than 99% and at least one of the identified peptides was there confirmed by a successful MS/MS analysis.

Additional measurements were carried out by means of a linear TOF-MS (AXIMA-LNR; Shimadzu Biotech-Kratos Analytical, Manchester, U.K.) using 2,4,6-trihydroxyacetophenone (Fluka; Buchs, Switzerland) as matrix and identical spotting procedure. A representative MS/MS spectrum and supplemental material to Tables 1 and 2 giving details of the MS and MS/MS protein identification results are included in Supporting Information.

Bioinformatics Data Analysis. The core data set for performing bioinformatics analysis of the proteomic data was defined by the list of identified proteins showing significantly different abundance between control and stressed group ("experimentally derived candidates"). Data processing included Principal Component Analysis (PCA) for identifying trends in the data sets potentially resting on the sequential setup of sample preparation for deriving biological replicates. One PCA component, explaining 8% of data variance, showed a correlation with cell line passages and was consequently removed from the data set. [33] Significance was derived by applying a t test for comparing the distribution of intensities of matched spots for the control group and the PDF stressed

group, each holding 16 samples. The significance level was set to 0.05. On the basis of inherent constraints of methodology and experimental design, the number of candidates is limited. Only proteins actually displayed on the gel and exhibiting large differences/small variances in the group comparison can be used for analyzing the given cellular condition. To overcome this limitation, a bioinformatic expansion of the experimentally derived candidates was performed.[34] Protein interaction networks (PINs) were generated utilizing the Online Predicted Human Interaction Database (OPHID).[35] OPHID provides information on interactions of the type protein A interacts with protein B. Processing a given protein list (A, B,..., N) with OPHID results in a set of undirected graphs representing the interactions between the proteins. A next neighbor X in the PIN is defined as A-X-B, where A and B are members of the candidate list, and X links A and B following the interaction data as given in OPHID. We expanded the list of experimentally determined candidates by the next neighbors from the PINs ("PIN derived candidates") resulting in an expanded list of candidates.[36,37]

For categorization of candidates in terms of biological processes, we used the PANTHER classification system.[38] Next to contextual grouping of a given protein list, PANTHER provides information on significant enrichment or depletion of the number of proteins assigned to a particular process by computing a Chi^2 test comparing the number of candidates belonging to a process and the total number of proteins assigned to this process as given by the PANTHER classification. Processes which were identified as significantly enriched or depleted only after next neighbor expansion, although no proteins of the experimentally derived candidate list were present in the respective biological process, were excluded.

Process Evaluation in Repeated Exposure Experiments. Proteins which were members of more than one biological processes were analyzed by using the VennMaster software (available from http://www.informatik.uni-ulm.de/ni/staff/HKestler/vennm/doc.html). Data lists holding candidate names and the respective biological process were used as input. The resulting Venn/Euler diagrams, where each circle represents a biological process, were optimized until all inconsistencies in the diagrams (missing overlaps) were eliminated. Overlapping areas in the diagrams represent candidates present in multiple biological processes. Processes exclusively containing proteins that are also in a significantly enriched parent process were omitted in the diagrams. ('Protein metabolism and modification' contains processes 'protein folding', 'protein modification', 'protein complex assembly' and 'stress response'. 'Cell cycle' contains 'cell cycle control'. 'Carbohydrate metabolism' contains 'glycolysis'. 'Cell structure and motility' contains 'cell structure'.)

Candidate Evaluation in Repeated Exposure Experiments. To analyze the protein expression pattern of selected candidates during repeated PDF exposure, differentially expressed candidates found in significantly enriched biological processes in the single exposure experiment were relocated in the gels prepared from the cell lysates following repeated PDF exposure. Candidates were classified as differentially expressed when their abundance ratio was either increased (>1.1) or decreased (<0.9) compared to the respective controls. Candidates which could not be allocated in the repeated exposure experiment or candidates with an abundance ratio between 0.9 and 1.1 in single exposure were excluded from this analysis. This selected candidate subset was characterized according to the number of enriched biological PANTHER processes to which they are assigned, and according to their abundance ratio in the repeated PDF exposure experiment. Abundance ratios from 0.9 to 1.1 in repeated exposure were categorized as "unchanged".

Results

Differential Abundance Analysis. In the single exposure experiment, 32 gels (16 controls, 16 "stressed", representing the 3 biological replicates and 5 to 6 technical replicates) showed a common spot pattern of 947 spots. Quantification revealed a set of 140 spots with altered abundance based on a significance level of $\alpha < 0.05$ (Figure 2). Eighty-two spots were found increased and 58 spots were found decreased relative to the control. Automated excision of all significantly changed spots allowed protein identification in 101 spots using MALDI-TOF MS and MS/MS techniques, where 12 identified proteins were present in 2 spots, 3 proteins were present in 3 spots and 1 protein was present in 4 spots. In total, 122 identifications holding 100 unique Swiss-Prot entry names could be assigned to significantly changed spots (Table 1).

In a second experiment aiming to determine the dynamics of protein expression after repeated exposure to PDF, cells were stressed twice. A single and a repeated exposure experiment were conducted in parallel both using adequate controls as described in Materials and Methods and shown in Figure 1. In the repeated exposure experiment, quantification revealed a set of 90 spots with altered abundance ($\alpha < 0.05$), where 44 spots were found increased and 46 spots were found decreased relative to the control. With the use of the tools described above, proteins were identified in 68 spots leading to 58 unique Swiss-Prot entry names (Table 2). For a number of candidates, quantification results were compared between 2DGE and Western blotting techniques demonstrating acceptable agreement, although the quantified species measured by 2DGE and identified by combined MS and MS/MS analysis might differ from the epitope recognized by a specific antibody as shown for the protein spots of HSPA1 and HSPB1 (Figure 3).

Mass Spectrometry. Protein identification was based on a combined database search, using MS as well as MS/MS data as described in Materials and Methods. The "Mascot protein score" reported in Tables 1 and 2 refers to this combined (MS and MS/MS data) database search. The "MS/MS ion score", given in addition in the supplemental table (Supporting Information), was calculated from the m/z values of fragment ions only using database searching without any previous manual or automated *de novo* sequencing procedure. The mass matching criteria for the MS and MS/MS modes was chosen as 75 ppm, a value offering sufficient tolerance to assign all peptide and fragment ions, respectively, in the spectrum originating from the sample. Taxonomy selection "mammals" was chosen to cover bovine proteins potentially present in the sample because of the feeding medium.

Analysis of Biological Processes. Bioinformatics utilizing the PANTHER protein classification on the basis of the experimentally derived candidate lists allowed an assignment to a biological process of all 100 proteins in the single exposure experiment and all 58 proteins in the repeated exposure experiment. Statistical analysis of the number of candidates found in the various processes revealed a significant overrepresentation (p-value <0.05) of the processes given in Table 3 during PDF stress response.

Table 1. Annotated Met5A Cell Proteins Showing Significant Differential Abundance after Single Exposure to PDF ($p < 0.05$)

protein name	ratio[a]	SD[b]	spot label[c]	no. of peptides[d]	Mascot protein score[e]	sequence coverage %	M_r[f]	pI[g]	Swiss-Prot entry name	protein symbol	NCBI gene ID	EC no.
Lamin-B1*	**1.81**	**0.65**	**46**	**28**	**467**	**50**	**66652.7**	**5.11**	**LMNB1_HUMAN**	**LMNB1**	**4001**	**n/a**
Neutral alpha-glucosidase AB*	**1.74**	**0.39**	**36**	**27**	**349**	**35**	**107262.8**	**5.74**	**GANAB_HUMAN**	**GANAB**	**23193**	**3.2.1.84**
Neutral alpha-glucosidase AB*	**1.64**	**0.31**	**38**	**37**	**540**	**48**	**107262.8**	**5.74**	**GANAB_HUMAN**	**GANAB**	**23193**	**3.2.1.84**
Beta-lactamase-like protein 2	1.52	0.28	82	10	229	39	33070.1	6.32	LACB2_HUMAN	LACTB2	212442	3.-.-.-
Elongation factor Ts, mitochondrial	1.47	0.19	42	11	328	42	35710.4	8.62	EFTS_HUMAN	TSFM	10102	n/a
Obg-like ATPase 1	1.43	0.18	10	17	378	52	44943.4	7.64	OLA1_HUMAN	OLA1	29789	3.6.3.-
Alpha-enolase*	**1.42**	**0.06**	**13**	**9**	**261**	**29**	**47481.4**	**7.01**	**ENOA_HUMAN**	ENO1	**2023**	**4.2.1.11**
Serpin H1*	**1.34**	**0.10**	**8**	**12**	**313**	**35**	**46525.2**	**8.75**	**SERPH_HUMAN**	**SERPINH1**	**871**	**n/a**
Heterogeneous nuclear ribonucleoprotein M	1.33	0.25	3	21	304	31	77749.4	8.84	HNRPM_HUMAN	HNRNPM	4670	n/a
Cytochrome c-type heme lyase*	**1.32**	**0.11**	**77**	**7**	**177**	**25**	**30981**	**6.25**	**CCHL_HUMAN**	**HCCS**	**3052**	**4.4.1.17**
Ubiquitin-conjugating enzyme E2 variant 1*	**1.32**	**0.09**	**89**	**9**	**210**	**45**	**26065.2**	**8.56**	**UB2V1_HUMAN**	**UBE2V1**	**7335**	**n/a**
Ubiquitin-conjugating enzyme E2 A*	**1.31**	**0.25**	**67**	**4**	**168**	**19**	**17418.6**	**5.06**	**UBE2A_HUMAN**	**UBE2A**	**7319**	**6.3.2.19**
Thioredoxin reductase 1, cytoplasmic	1.31	0.19	7	14	199	32	55470.2	6.07	TRXR1_HUMAN	TXNRD1	7296	1.8.1.9
T-complex protein 1 subunit eta*	**1.30**	**0.10**	**15**	**15**	**290**	**39**	**59798.1**	**7.55**	**TCPH_HUMAN**	**CCT7**	**10574**	**n/a**
GTP:AMP phosphotransferase mitochondrial	1.29	0.17	100	11	324	51	25549.6	9.15	KAD3_HUMAN	AK3	50808	2.7.4.10
Secernin-1	1.29	0.23	54	13	262	39	46979.8	4.66	SCRN1_HUMAN	SCRN1	9805	n/a
26S proteasome non-ATPase regulatory subunit 4*	**1.29**	**0.23**	**54**	**12**	**144**	**40**	**40939.3**	**4.68**	**PSMD4_HUMAN**	**PSMD4**	**5710**	**n/a**
Actin, cytoplasmic 1*	**1.28**	**0.09**	**58**	**11**	**367**	**42**	**42067.9**	**5.3**	**ACTB_HUMAN**	**ACTB**	**60**	**n/a**
Voltage-dependent anion-selective channel protein 2	1.28	0.10	90	10	236	44	32073.8	7.49	VDAC2_HUMAN	VDAC2	7417	n/a
Serine-threonine kinase receptor-associated protein*	**1.27**	**0.09**	**57**	**13**	**287**	**50**	**38756.1**	**4.98**	**STRAP_HUMAN**	**STRAP**	**11171**	**n/a**
Bifunctional 3′-phosphoadenosine 5′-phosphosulfate	1.27	0.13	9	8	155	14	70026.8	8.18	PAPS2_HUMAN	PAPSS2	9060	n/a
Voltage-dependent anion-selective channel protein 3	1.27	0.14	99	10	319	44	30981.4	8.85	VDAC3_HUMAN	VDAC3	7419	n/a
Alpha-enolase*	**1.26**	**0.16**	**23**	**17**	**353**	**50**	**47481.4**	**7.01**	**ENOA_HUMAN**	**ENO1**	**2023**	**4.2.1.11**
Phosphoglycerate mutase 1*	**1.26**	**0.07**	**79**	**12**	**266**	**55**	**28927.9**	**6.67**	**PGAM1_HUMAN**	**PGAM1**	**5223**	**5.4.2.1**
Protein-L-isoaspartate-(D-aspartate)*	**1.24**	**0.02**	**75**	**7**	**147**	**28**	**24777.6**	**6.7**	**PIMT_HUMAN**	**PCMT1**	**5110**	**2.1.1.77**
Protein NipSnap1*	**1.24**	**0.15**	**101**	**10**	**150**	**36**	**33459.9**	**9.35**	**NIPS1_HUMAN**	**NIPSNAP1**	**8508**	**n/a**
Growth factor receptor-bound protein 2*	**1.23**	**0.02**	**74**	**11**	**297**	**57**	**25304.5**	**5.89**	**GRB2_HUMAN**	**GRB2**	**2885**	**n/a**
Alpha-centractin*	**1.23**	**0.09**	**22**	**12**	**292**	**39**	**42700.9**	**6.19**	**ACTZ_HUMAN**	**ACTR1A**	**10121**	**n/a**
Aminoacylase-1	1.23	0.12	73	10	186	31	46084.1	5.77	ACY1_HUMAN	ACY1	95	3.5.1.14
Protein phosphatase methylesterase 1*	**1.23**	**0.12**	**73**	**10**	**132**	**26**	**42629.3**	**5.77**	**PPME1_HUMAN**	**PPME1**	**51400**	**3.1.1.-**
Tubulin folding cofactor B*	**1.22**	**0.04**	**64**	**11**	**470**	**54**	**27593.6**	**5.06**	**TBCB_HUMAN**	**TBCB**	**1155**	**n/a**
F-actin-capping protein subunit alpha-2*	**1.22**	**0.14**	**71**	**11**	**322**	**54**	**33156.7**	**5.57**	**CAZA2_HUMAN**	**CAPZA2**	**830**	**n/a**
Medium-chain specific acyl-CoA dehydrogenase	1.22	0.05	18	11	178	29	47033.8	8.61	ACADM_HUMAN	ACADM	34	1.3.99.3
Endoplasmin, Heat shock protein 90 kDa beta member 1*	**1.22**	**0.04**	**49**	**26**	**523**	**33**	**92840.5**	**4.76**	**ENPL_HUMAN**	**HSP90B1**	**7184**	**n/a**
Keratin, type II cytoskeletal 7*	**1.22**	**0.10**	**43**	**20**	**345**	**45**	**51443.4**	**5.5**	**K2C7_HUMAN**	**KRT7**	**3855**	**n/a**
Golgi reassembly stacking protein 2	1.21	0.11	53	5	111	11	47287.1	4.73	GORS2_HUMAN	GORASP2	26003	n/a
Adenosylhomocysteinase	1.21	0.07	29	22	432	54	48255.4	5.92	SAHH_HUMAN	AHCY	191	3.3.1.1
Transaldolase*	**1.21**	**0.04**	**80**	**13**	**216**	**37**	**37687.5**	**6.36**	**TALDO_HUMAN**	**TALDO1**	**6888**	**2.2.1.2**
Pyruvate kinase isozymes M1/M2*	**1.21**	**0.05**	**12**	**15**	**256**	**39**	**58470.2**	**7.96**	**KPYM_HUMAN**	**PKM2**	**5315**	**2.7.1.40**
Heat shock 70 kDa protein 4*	**1.19**	**0.01**	**44**	**28**	**600**	**47**	**95095.6**	**5.18**	**HSP74_HUMAN**	**HSPA4**	**3308**	**n/a**

Table 1. Continued

protein name	ratio[a]	SD[b]	spot label[c]	no. of peptides[d]	Mascot protein score[e]	sequence coverage %	M_r[f]	p*I*[g]	Swiss-Prot entry name	protein symbol	NCBI gene ID	EC no.
Proteasome subunit beta type-3	1.19	0.03	76	9	326	41	23262.6	6.15	PSB3_HUMAN	PSMB3	5691	3.4.25.1
5′(3′)-deoxyribonucleotidase, cytosolic type	1.19	0.03	76	11	164	60	23596.2	6.18	NT5C_HUMAN	NT5C	30833	3.1.3.-
Alpha-enolase*	**1.18**	**0.07**	**16**	**15**	**441**	**42**	**47481.4**	**7.01**	**ENOA_HUMAN**	**ENO1**	**2023**	**4.2.1.11**
ATP synthase subunit alpha, mitochondrial	1.18	0.06	11	19	484	42	59827.6	9.16	ATPA_HUMAN	ATP5A1	498	n/a
Actin, cytoplasmic 1*	**1.17**	**0.05**	**48**	**9**	**343**	**34**	**42081.9**	**5.3**	**ACTB_HUMAN**	**ACTB**	**60**	**n/a**
Heterogeneous nuclear ribonucleoprotein L	1.17	0.11	20	14	198	32	60719.4	6.65	HNRPL_HUMAN	HNRNPL	3191	n/a
Peptidyl-prolyl *cis*−*trans* isomerase A*	**1.17**	**0.04**	**88**	**5**	**227**	**34**	**18229**	**7.68**	**PPIA_HUMAN**	**PPIA**	**5478**	**5.2.1.8**
Thioredoxin reductase 1, cytoplasmic	1.16	0.11	28	17	362	38	55470.2	6.07	TRXR1_HUMAN	TXNRD1	7296	1.8.1.9
T-complex protein 1 subunit beta*	**1.16**	**0.11**	**28**	**16**	**246**	**45**	**57794.3**	**6.01**	**TCPB_HUMAN**	**CCT2**	**10576**	**n/a**
Lamin-A/C*	**1.16**	**0.13**	**27**	**23**	**198**	**34**	**74379.8**	**6.57**	**LMNA_HUMAN**	**LMNA**	**4000**	**n/a**
Bifunctional purine biosynthesis protein PURH	1.16	0.13	27	12	141	28	65165.7	6.42	PUR9_HUMAN	ATIC	471	n/a
60 kDa heat shock protein, mitochondrial*	**1.16**	**0.05**	**45**	**22**	**547**	**48**	**61187.4**	**5.7**	**CH60_HUMAN**	**HSPD1**	**3329**	**n/a**
Inosine-5′-monophosphate dehydrogenase 2	1.15	0.04	21	14	283	30	56225.8	6.44	IMDH2_HUMAN	IMPDH2	3615	1.1.1.205
Glucose-6-phosphate 1-dehydrogenase*	**1.15**	**0.04**	**21**	**12**	**170**	**23**	**59675.2**	**6.39**	**G6PD_HUMAN**	**G6PD**	**2539**	**1.1.1.49**
Voltage-dependent anion-selective channel protein 2	1.15	0.03	86	9	319	44	32073.8	7.49	VDAC2_HUMAN	VDAC2	7417	n/a
Glutamate dehydrogenase 1, mitochondrial	1.14	0.06	19	25	523	51	61701.3	7.66	DHE3_HUMAN	GLUD1	2746	1.4.1.3
Heat shock cognate 71 kDa protein*	**1.14**	**0.02**	**41**	**16**	**331**	**30**	**71055.3**	**5.37**	**HSP7C_HUMAN**	**HSPA8**	**3312**	**n/a**
Stress-70 protein, mitochondrial*	**1.14**	**0.02**	**41**	**15**	**241**	**29**	**73929.9**	**5.81**	**GRP75_HUMAN**	**HSPA9**	**3313**	**n/a**
Chloride intracellular channel protein 4	1.14	0.04	69	11	392	50	28981.8	5.45	CLIC4_HUMAN	CLIC4	25932	n/a
Proteasome inhibitor PI31 subunit	1.14	0.04	69	7	134	35	29956	5.4	PSMF1_HUMAN	PSMF1	9491	n/a
Lamin-A/C*	**1.14**	**0.02**	**24**	**31**	**348**	**47**	**74379.8**	**6.57**	**LMNA_HUMAN**	**LMNA**	**4000**	**n/a**
Bifunctional purine biosynthesis protein PURH	1.14	0.02	24	18	257	39	65088.5	6.27	PUR9_HUMAN	ATIC	471	n/a
Lactoylglutathione lyase	1.14	0.04	68	7	274	36	20992.3	5.12	LGUL_HUMAN	GLO1	2739	4.4.1.5
GTP-binding nuclear protein Ran*	**1.14**	**0.08**	**87**	**13**	**384**	**54**	**24582.7**	**7.7**	**RAN_HUMAN**	**RAN**	**5901**	**n/a**
Acetyl-CoA acetyltransferase, cytosolic*	**1.13**	**0.01**	**83**	**10**	**366**	**40**	**41837.6**	**6.47**	**THIC_HUMAN**	**ACAT2**	**39**	**2.3.1.9**
Twinfilin-2*	**1.13**	**0.01**	**83**	**10**	**243**	**42**	**39751.4**	**6.37**	**TWF2_HUMAN**	**TWF2**	**11344**	**n/a**
RNA-binding protein 4	1.13	0.01	83	10	167	38	40687.8	6.61	RBM4_HUMAN	RBM4	5936	n/a
Heat shock 70 kDa protein 1*	**1.12**	**0.01**	**39**	**19**	**388**	**38**	**70294.1**	**5.48**	**HSP71_HUMAN**	**HSPA1A**	**3303**	**n/a**
Alpha-enolase*	**1.12**	**0.02**	**17**	**12**	**310**	**41**	**47481.4**	**7.01**	**ENOA_HUMAN**	**ENO1**	**2023**	**4.2.1.11**
Triosephosphate isomerase*	**1.12**	**0.04**	**85**	**10**	**267**	**48**	**26937.8**	**6.45**	**TPIS_HUMAN**	**TPI1**	**7167**	**5.3.1.1**
Proteasome subunit alpha type-2*	**1.12**	**0.04**	**85**	**8**	**257**	**52**	**25996.3**	**6.92**	**PSA2_HUMAN**	**PSMA2**	**5683**	**3.4.25.1**
Protein-L-isoaspartate-(D-aspartate)*	**1.12**	**0.04**	**85**	**6**	**121**	**28**	**24792.6**	**6.23**	**PIMT_HUMAN**	**PCMT1**	**5110**	**2.1.1.77**
Macrophage-capping protein*	**1.12**	**0.02**	**30**	**4**	**202**	**15**	**38778.6**	**5.88**	**CAPG_HUMAN**	**CAPG**	**822**	**n/a**
Tropomyosin alpha-3 chain*	**1.12**	**0.01**	**63**	**10**	**175**	**21**	**32899.8**	**4.68**	**TPM3_HUMAN**	**TPM3**	**7170**	**n/a**
14-3-3 protein epsilon*	**1.12**	**0.01**	**62**	**8**	**108**	**36**	**29326.5**	**4.63**	**1433E_HUMAN**	**YWHAE**	**7531**	**n/a**
Fructose-bisphosphate aldolase A*	**1.11**	**0.02**	**93**	**16**	**460**	**64**	**39851.5**	**8.3**	**ALDOA_HUMAN**	**ALDOA**	**226**	**4.1.2.13**
Myosin regulatory light chain 2, smooth muscle isoform*	**1.11**	**0.01**	**66**	**4**	**83**	**24**	**19871.5**	**4.8**	**MLRN_HUMAN**	**MYL9**	**10398**	**n/a**
Myosin regulatory light chain 2, nonsarcomeric*	**1.10**	**0.05**	**65**	**5**	**145**	**36**	**19838.5**	**4.67**	**MLRM_HUMAN**	**MRLC3**	**10627**	**n/a**
Fructose-bisphosphate aldolase A*	**1.10**	**0.05**	**65**	**7**	**133**	**29**	**39865.5**	**8.3**	**ALDOA_HUMAN**	**ALDOA**	**226**	**4.1.2.13**
Heterogeneous nuclear ribonucleoprotein A3	1.10	0.05	1	13	276	35	39855.7	9.1	ROA3_HUMAN	HNRNPA3	220988	n/a
Aspartate aminotransferase, mitochondrial	1.10	0.05	1	12	184	40	47844.4	9.14	AATM_HUMAN	GOT2	2806	2.6.1.1
Keratin, type II cytoskeletal 8*	**1.09**	**0.01**	**37**	**21**	**339**	**42**	**53671.1**	**5.52**	**K2C8_HUMAN**	**KRT8**	**3856**	**n/a**

Table 1. Continued

protein name	ratio[a]	SD[b]	spot label[c]	no. of peptides[d]	Mascot protein score[e]	sequence coverage %	M_r[f]	p*I*[g]	Swiss-Prot entry name	protein symbol	NCBI gene ID	EC no.
NAD(P)H dehydrogenase [quinone] 1	1.09	0.05	97	9	226	26	30977.1	8.72	NQO1_HUMAN	NQO1	1728	1.6.5.2
Carbonyl reductase [NADPH] 1	1.09	0.05	97	12	222	59	30656.9	8.56	CBR1_HUMAN	CBR1	873	n/a
Tropomyosin alpha-1 chain*	**1.08**	**0.02**	**60**	**16**	**285**	**36**	**32745.7**	**4.69**	**TPM1_HUMAN**	**TPM1**	**7168**	**n/a**
Peroxiredoxin-1*	**1.08**	**0.09**	**95**	**6**	**204**	**38**	**22324.4**	**8.27**	**PRDX1_HUMAN**	**PRDX1**	**5052**	**1.11.1.15**
Isocitrate dehydrogenase [NADP] cytoplasmic*	**0.91**	**0.05**	**84**	**10**	**206**	**29**	**46914.6**	**6.53**	**IDHC_HUMAN**	**IDH1**	**3417**	**1.1.1.42**
Heterogeneous nuclear ribonucleoprotein M	0.90	0.12	4	20	284	32	77749.4	8.84	HNRPM_HUMAN	HNRNPM	4670	n/a
Heterogeneous nuclear ribonucleoproteins A2/B1	0.89	0.03	94	13	284	45	37436.7	8.97	ROA2_HUMAN	HNRNPA2B1	3181	n/a
Fumarate hydratase, mitochondrial	0.89	0.15	14	10	403	22	54773.2	8.85	FUMH_HUMAN	FH	2271	4.2.1.2
Complement component 1 Q subcomponent-binding*	**0.87**	**0.06**	**59**	**6**	**325**	**40**	**31741.8**	**4.74**	**C1QBP_HUMAN**	**C1QBP**	**708**	**n/a**
14-3-3 protein epsilon*	**0.87**	**0.14**	**61**	**6**	**98**	**28**	**29326.5**	**4.63**	**1433E_HUMAN**	**YWHAE**	**7531**	**n/a**
Annexin A2*	**0.87**	**0.03**	**47**	**17**	**319**	**45**	**38807.9**	**7.57**	**ANXA2_HUMAN**	**ANXA2**	**302**	**n/a**
Heterogeneous nuclear ribonucleoprotein A/B	0.87	0.03	47	8	171	27	36316.4	8.22	ROAA_HUMAN	HNRNPAB	3182	n/a
UPF0160 protein MYG1	0.81	0.15	31	8	151	25	42760.6	6.25	MYG1_HUMAN	C12orf10	60314	n/a
Protein disulfide-isomerase A3*	**0.80**	**0.13**	**70**	**23**	**448**	**49**	**57145.9**	**5.98**	**PDIA3_HUMAN**	**PDIA3**	**2923**	**5.3.4.1**
Immunity-related GTPase family Q protein	0.80	0.17	51	9	181	17	63191.6	4.81	IRGQ_HUMAN	IRGQ	126298	n/a
Neutral alpha-glucosidase AB*	**0.80**	**0.11**	**32**	**14**	**151**	**16**	**107262.8**	**5.74**	**GANAB_HUMAN**	**GANAB**	**23193**	**3.2.1.84**
Trifunctional enzyme subunit alpha, mitochondrial*	**0.79**	**0.11**	**2**	**21**	**277**	**31**	**83688.1**	**9.16**	**ECHA_HUMAN**	**HADHA**	**3030**	**n/a**
Probable ATP-dependent RNA helicase DDX17	0.78	0.11	5	11	146	17	72981.2	8.82	DDX17_HUMAN	DDX17	10521	3.6.1.-
Actin, cytoplasmic 1*	**0.77**	**0.19**	**50**	**9**	**179**	**36**	**42051.9**	**5.29**	**ACTB_HUMAN**	**ACTB**	**60**	**n/a**
Annexin A2*	**0.77**	**0.03**	**91**	**10**	**201**	**27**	**38807.9**	**7.57**	**ANXA2_HUMAN**	**ANXA2**	**302**	**n/a**
Heterogeneous nuclear ribonucleoprotein A/B	0.77	0.03	91	9	121	20	36316.4	8.22	ROAA_HUMAN	HNRNPAB	3182	n/a
Protein C14orf166*	**0.76**	**0.02**	**78**	**14**	**454**	**62**	**28164.8**	**6.19**	**CN166_HUMAN**	**C14orf166**	**51637**	**n/a**
Cleavage and polyadenylation specificity factor subunit	0.76	0.06	96	7	231	30	26267.8	8.85	CPSF5_HUMAN	NUDT21	11051	n/a
Guanine nucleotide-binding protein subunit beta-2-like 1*	**0.75**	**0.04**	**92**	**15**	**445**	**57**	**35510.7**	**7.6**	**GBLP_HUMAN**	**GNB2L1**	**10399**	**n/a**
Heat shock 70 kDa protein 1*	**0.75**	**0.03**	**40**	**24**	**475**	**49**	**70294.1**	**5.48**	**HSP71_HUMAN**	**HSPA1A**	**3303**	**n/a**
Heat shock protein beta-1*	**0.75**	**0.13**	**72**	**12**	**279**	**51**	**22825.5**	**5.98**	**HSPB1_HUMAN**	**HSPB1**	**3315**	**n/a**
Poly(rC)-binding protein 2	0.73	0.01	81	9	206	37	38954.7	6.33	PCBP2_HUMAN	PCBP2	5094	n/a
Protein disulfide-isomerase*	**0.71**	**0.05**	**52**	**23**	**525**	**46**	**57479.8**	**4.76**	**PDIA1_HUMAN**	**P4HB**	**5034**	**5.3.4.1**
Transgelin	0.70	0.06	98	12	282	58	22653.4	8.87	TAGL_HUMAN	TAGLN	6876	n/a
Gelsolin*	**0.70**	**0.13**	**35**	**12**	**206**	**20**	**86043.3**	**5.9**	**GELS_HUMAN**	**GSN**	**2934**	**n/a**
Radixin*	**0.69**	**0.09**	**26**	**14**	**278**	**24**	**68621.4**	**5.95**	**RADI_HUMAN**	**RDX**	**5962**	**n/a**
Moesin*	**0.69**	**0.09**	**26**	**6**	**188**	**10**	**67867.9**	**6.16**	**MOES_HUMAN**	**MSN**	**4478**	**n/a**
Ezrin*	**0.69**	**0.09**	**26**	**5**	**177**	**6**	**69483.8**	**5.94**	**EZRI_HUMAN**	**EZR**	**7430**	**n/a**
Procollagen-lysine,2-oxoglutarate 5-dioxygenase 3	0.68	0.17	33	15	246	21	85301.7	5.74	PLOD3_HUMAN	PLOD3	8985	1.14.11.4
GMP synthase [glutamine-hydrolyzing]	0.68	0.09	25	20	270	38	77408.2	6.42	GUAA_HUMAN	GMPS	8833	6.3.5.2
Lamin-A/C*	**0.68**	**0.09**	**25**	**23**	**256**	**38**	**74379.8**	**6.57**	**LMNA_HUMAN**	**LMNA**	**4000**	**n/a**
Ribonuclease inhibitor	0.67	0.05	56	14	258	50	51765.8	4.71	RINI_HUMAN	RNH1	6050	n/a
Ribonuclease inhibitor	0.62	0.07	55	12	258	35	51765.8	4.71	RINI_HUMAN	RNH1	6050	n/a
Serpin H1*	**0.55**	**0.05**	**6**	**3**	**84**	**9**	**46525.2**	**8.75**	**SERPH_HUMAN**	**SERPINH1**	**871**	**n/a**

[a] Ratio: Fold-change of spot abundance of stressed cells vs control cells in the single exposure experiment. [b] SD: Standard deviation of the quantification data. [c] Spot label of the respective protein in Figure 2. [d] Number of peptides matching in the peptide mass fingerprint based identification. [e] Mascot Protein Score: obtained from the combined (MS + MS/MS data) database search. [f] Relative molecular mass of the protein as calculated from the amino acid sequence of the polypeptide without any co- or post-translational modifications. [g] Calculated p*I* of the polypeptide as obtained from Swiss-Prot database. Proteins indicated by asterisks (bold rows) were found in significantly overrepresented biological processes following the PANTHER classification system.

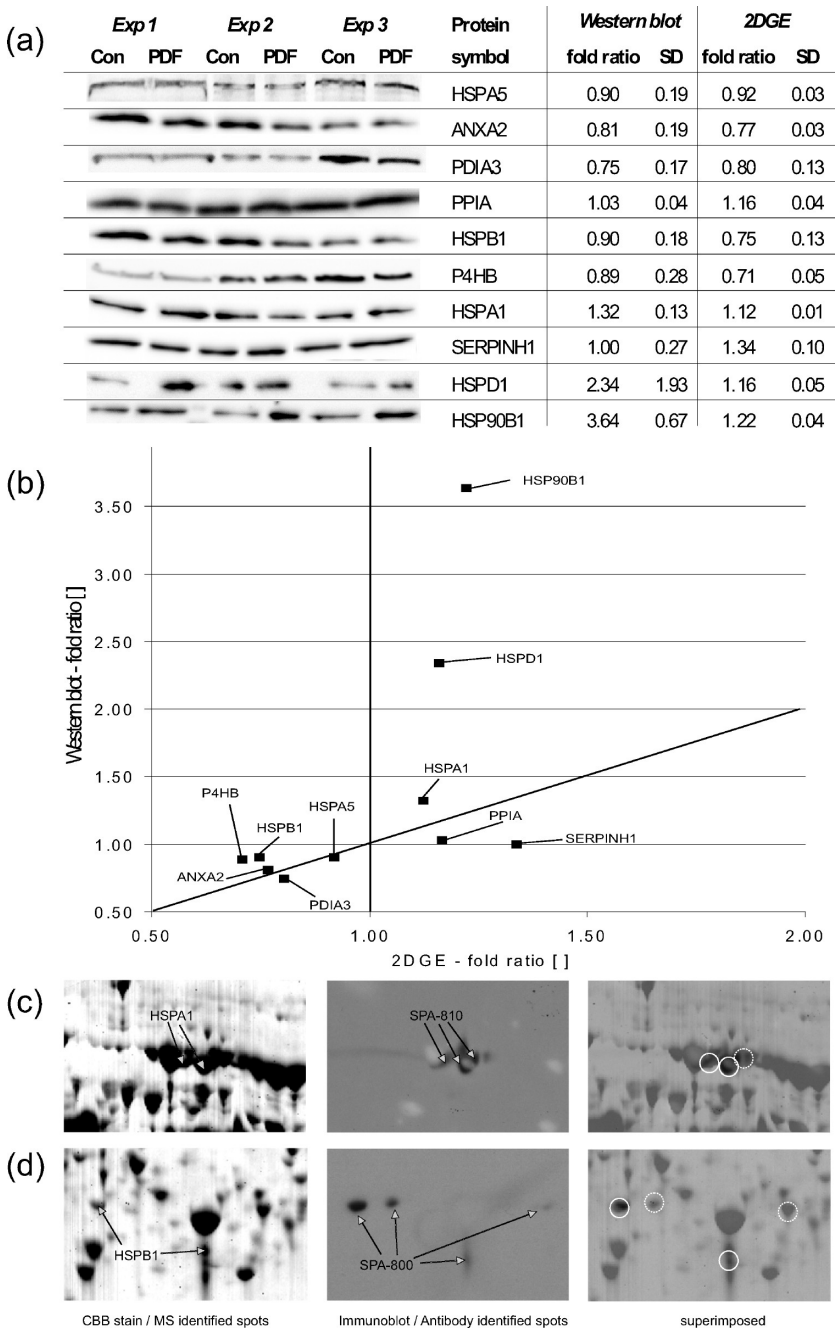

Figure 3. Western blots of selected proteins found differentially abundant after PDF exposure. (a) Relevant regions from Western blots using specific antibodies for the proteins listed and comparison of fold change ratios and standard deviations (SD) as measured by Western blot and 2DGE. (b) Graphical comparison of densitometric data from Western blot and 2DGE as given in panel a. (c) 2D gels and immunoblots of the HSPA1 region. The left panel shows the Coomassie brilliant blue (CBB) stained gel and the MS identified protein spots. The middle panel shows the result of the immunoblot with positive signals indicated by arrows and the specific antibody SPA-810. The right panel shows superposition of the CBB stained gel and the immunoblot with solid circles indicating doubly identified proteins and broken circles indicating spots that were identified only by immunoblot. (d) Analogue representation as panel c for HSPB1.

Naturally, substantial coverage of single biological processes on the level of 100 candidates in the single exposure experiment, or 58 candidates in the repeated exposure experiment cannot be expected. Therefore, expansions of these given lists based on available biological data on protein interactions were performed.

Protein-Interaction Network Analysis. Investigating the protein interaction network (PIN) on the basis of the 100 experimentally identified candidates in single exposure applying OPHID data resulted in a graph holding 81 protein nodes and 16 protein interaction edges. The remaining 19 candidates were not listed in OPHID. The largest subgraph showed 7 members of the candidate list interlinked by six protein interaction edges as given in the OPHID data set. Only nine additional protein interactions were found between the other protein nodes indicating no (known) direct interactions between these candidates. Expanding the list of 81 experimentally determined candidates also represented in OPHID by utilizing

Table 2. Annotated Met5A Cell Proteins Showing Significant Differential Abundance after Repeated Exposure to PDF ($p < 0.05$)

protein name	ratio[a]	SD[b]	no. of peptides[c]	Mascot protein score[d]	sequence coverage %	M_r[e]	pI[f]	Swiss-Prot entry name	protein symbol	NCBI gene ID	EC no.
Cysteine and glycine-rich protein 1*	**5.16**	**1.59**	**5**	**174**	**35**	**21409.1**	**8.9**	**CSRP1_HUMAN**	**CSRP1**	**1465**	**n/a**
Proteasome subunit beta type 6 precursor	3.45	0.83	7	195	19	25569.5	4.8	PSB6_HUMAN	PSMB6	5694	3.4.25.1
Ubiquitin-conjugating enzyme E2 N*	**3.26**	**0.39**	**9**	**422**	**38**	**17184**	**6.13**	**UBE2N_HUMAN**	**UBE2N**	**7334**	**6.3.2.19**
Proteasome subunit beta type 2	3.04	0.52	9	171	37	22992.7	6.51	PSB2_HUMAN	PSMB2	5690	3.4.25.1
Splicing factor, arginine/serine-rich 1*	**2.91**	**0.71**	**7**	**127**	**27**	**27841.9**	**10.37**	**SFRS1_HUMAN**	**SFRS1**	**6426**	**n/a**
RNA-binding protein 8A*	**2.70**	**0.47**	**4**	**129**	**18**	**19933.8**	**5.5**	**RBM8A_HUMAN**	**RBM8A**	**9939**	**n/a**
Serpin B9	2.10	0.44	9	158	21	43003.5	5.61	SPB9_HUMAN	SERPINB9	5272	n/a
T-complex protein 1 subunit epsilon	2.02	0.65	19	358	41	60089	5.45	TCPE_HUMAN	CCT5	22948	n/a
DNA replication licensing factor MCM4*	**1.95**	**0.27**	**10**	**124**	**10**	**97067.8**	**6.28**	**MCM4_HUMAN**	**MCM4**	**4173**	**n/a**
Adenylate kinase isoenzyme 2, mitochondrial*	**1.93**	**0.49**	**4**	**111**	**20**	**26688.9**	**7.67**	**KAD2_HUMAN**	**AK2**	**204**	**2.7.4.3**
Prefoldin subunit 5	1.88	0.32	5	111	28	17374	5.93	PFD5_HUMAN	PFDN5	5204	n/a
Heterogeneous nuclear ribonucleoprotein M*	**1.78**	**0.57**	**14**	**134**	**21**	**77749.4**	**8.84**	**HNRPM_HUMAN**	**HNRNPM**	**4670**	**n/a**
Protein C14orf166	1.75	0.17	14	454	72	28164.8	6.19	CN166_HUMAN	C14orf166	51637	n/a
Iron-responsive element-binding protein 1*	**1.64**	**0.17**	**7**	**113**	**6**	**98849.8**	**6.23**	**IREB1_HUMAN**	**ACO1**	**48**	**4.2.1.3**
Cofilin-2*	**1.57**	**0.24**	**4**	**162**	**31**	**18838.9**	**7.66**	**COF2_HUMAN**	**CFL2**	**1073**	**n/a**
Ribonuclease inhibitor	1.57	0.21	8	114	24	51765.8	4.71	RINI_HUMAN	RNH1	6050	n/a
Glyoxylate reductase/hydroxypyruvate reductase	1.52	0.23	5	80	18	36044.9	7.01	GRHPR_HUMAN	GRHPR	9380	1.1.1.79
Proliferating cell nuclear antigen*	**1.34**	**0.18**	**6**	**168**	**20**	**29092.4**	**4.57**	**PCNA_HUMAN**	**PCNA**	**5111**	**n/a**
ADP-ribosylation factor-like protein 3	1.32	0.14	3	77	26	20613.8	6.74	ARL3_HUMAN	ARL3	403	n/a
Heat shock protein beta-1*	1.30	0.09	9	510	48	22825.5	5.98	HSPB1_HUMAN	HSPB1	3315	n/a
Profilin-2*	**1.28**	**0.08**	**2**	**166**	**11**	**15378.4**	**6.55**	**PROF2_HUMAN**	**PFN2**	**5217**	**n/a**
Phosphatidylethanolamine-binding protein 1	1.26	0.02	15	719	82	21157.7	7.01	PEBP1_HUMAN	PEBP1	5037	n/a
Destrin*	**1.26**	**0.03**	**6**	**112**	**33**	**18506.4**	**8.12**	**DEST_HUMAN**	**DSTN**	**11034**	**n/a**
Macrophage migration inhibitory factor*	**1.25**	**0.07**	**5**	**126**	**36**	**12639.3**	**7.74**	**MIF_HUMAN**	**MIF**	**4282**	**5.3.2.1**
Macrophage migration inhibitory factor*	**1.23**	**0.06**	**3**	**117**	**23**	**12639.3**	**7.74**	**MIF_HUMAN**	**MIF**	**4282**	**5.3.2.1**
Glutathione S-transferase P*	**1.22**	**0.07**	**6**	**212**	**36**	**23569.1**	**5.43**	**GSTP1_HUMAN**	**GSTP1**	**2950**	**2.5.1.18**
Actin, cytoplasmic 2*	**1.21**	**0.04**	**21**	**624**	**60**	**42107.9**	**5.31**	**ACTG_HUMAN**	**ACTG1**	**71**	**n/a**
Heterogeneous nuclear ribonucleoprotein K*	**1.16**	**0.04**	**11**	**175**	**30**	**51229.5**	**5.39**	**HNRPK_HUMAN**	**HNRNPK**	**3190**	**n/a**
Probable ATP-dependent RNA helicase DDX5*	**1.15**	**0.03**	**25**	**395**	**40**	**69617.9**	**9.06**	**DDX5_HUMAN**	**DDX5**	**1655**	**3.6.1.-**
40S ribosomal protein SA	0.95	0.02	10	412	40	32947.5	4.79	RSSA_HUMAN	RPSA	3921	n/a
78 kDa glucose-regulated protein precursor*	**0.91**	**0.03**	**25**	**447**	**43**	**72402.5**	**5.07**	**GRP78_HUMAN**	**HSPA5**	**3309**	**n/a**
Triosephosphate isomerase*	**0.90**	**0.02**	**20**	**724**	**83**	**26937.8**	**6.45**	**TPIS_HUMAN**	**TPI1**	**7167**	**5.3.1.1**
Triosephosphate isomerase*	**0.87**	**0.02**	**10**	**117**	**42**	**26937.8**	**6.45**	**TPIS_HUMAN**	**TPI1**	**7167**	**5.3.1.1**
Proteasome subunit alpha type 2	0.87	0.02	10	211	44	25996.3	6.92	PSA2_HUMAN	PSMA2	5683	3.4.25.1
Glyceraldehyde-3-phosphate dehydrogenase	0.87	0.02	5	202	18	36201.5	8.57	G3P_HUMAN	GAPDH	2597	1.2.1.12
Actin, cytoplasmic 2*	**0.87**	**0.02**	**11**	**306**	**29**	**42107.9**	**5.31**	**ACTG_HUMAN**	**ACTG1**	**71**	**n/a**
Proliferating cell nuclear antigen*	**0.87**	**0.03**	**10**	**340**	**42**	**29092.4**	**4.57**	**PCNA_HUMAN**	**PCNA**	**5111**	**n/a**
Proliferating cell nuclear antigen*	**0.85**	**0.05**	**6**	**119**	**15**	**29092.4**	**4.57**	**PCNA_HUMAN**	**PCNA**	**5111**	**n/a**
Annexin A11	0.83	0.05	2	73	5	54697.2	7.53	ANX11_HUMAN	ANXA11	311	n/a
Glucose-6-phosphate 1-dehydrogenase*	**0.83**	**0.05**	**5**	**82**	**9**	**59675.2**	**6.39**	**G6PD_HUMAN**	**G6PD**	**2539**	**1.1.1.49**
Inosine-5′-monophosphate dehydrogenase 2*	**0.83**	**0.05**	**6**	**123**	**13**	**56225.8**	**6.44**	**IMDH2_HUMAN**	**IMPDH2**	**3615**	**1.1.1.205**
Protein MEMO1	0.83	0.06	8	210	23	34110.6	6.67	MEMO1_HUMAN	MEMO1	51072	n/a

Table 2. Continued

protein name	ratio[a]	SD[b]	no. of peptides[c]	Mascot protein score[d]	sequence coverage %	M_r[e]	p*I*[f]	Swiss-Prot entry name	protein symbol	NCBI gene ID	EC no.
Pyruvate dehydrogenase E1 component subunit beta*	**0.83**	**0.04**	**4**	**132**	**10**	**39550.2**	**6.2**	**ODPB_HUMAN**	**PDHB**	**5162**	**1.2.4.1**
Guanine nucleotide-binding protein G(I)/G(S)/G(T)	0.83	0.04	10	147	26	38048.3	5.6	GBB1_HUMAN	GNB1	2782	n/a
F-actin-capping protein subunit alpha-1*	0.83	**0.04**	**10**	**134**	**41**	**33073.4**	**5.45**	**CAZA1_HUMAN**	**CAPZA1**	**829**	**n/a**
Guanine nucleotide-binding protein G(I)/G(S)/G(T)	0.81	0.06	8	284	22	38151.3	5.6	GBB1_HUMAN	GNB1	2782	n/a
Uncharacterized protein C20orf77	0.80	0.06	6	141	25	36991.2	5.73	CT077_HUMAN	C20orf77	58490	n/a
Proto-oncogene C-crk	0.80	0.06	11	210	46	33867	5.38	CRK_HUMAN	CRK	1398	n/a
BTB/POZ domain-containing protein KCTD12	0.80	0.06	16	179	43	35963.8	5.51	KCD12_HUMAN	KCTD12	115207	n/a
Ubiquinol-cytochrome c reductase iron−sulfur subunit	0.80	0.07	6	82	17	29934.5	8.55	UCRI_HUMAN	UQCRFS1	7386	1.10.2.2
Delta(3,5)-Delta(2,4)-dienoyl-CoA isomerase*	0.79	0.05	**4**	**110**	**32**	**36105.5**	**8.16**	**ECH1_HUMAN**	**ECH1**	**1891**	**5.3.3.-**
Protein SEC13 homologue*	**0.79**	**0.07**	**10**	**288**	**33**	**36031.3**	**5.22**	**nSEC13_HUMAN**	**SEC13**	**6396**	**n/a**
Thioredoxin reductase 1, cytoplasmic precursor	0.76	0.08	13	199	33	55470.2	6.07	TRXR1_HUMAN	TXNRD1	7296	1.8.1.9
Actin, cytoplasmic 2*	**0.76**	**0.07**	**11**	**314**	**35**	**42107.9**	**5.31**	**ACTG_HUMAN**	**ACTG1**	**71**	**n/a**
Interferon-induced 17 kDa protein precursor	0.76	0.06	5	138	17	17933.4	6.84	UCRP_HUMAN	ISG15	9636	n/a
Actin, cytoplasmic 2*	**0.75**	**0.05**	**8**	**118**	**28**	**42107.9**	**5.31**	**ACTG_HUMAN**	**ACTG1**	**71**	**n/a**
tRNA (adenine-N(1)-)-methyltransferase catalytic subunit TRM61*	**0.75**	**0.09**	**3**	**78**	**15**	**31704**	**6.89**	**TRM61_HUMAN**	**TRM61**	**115708**	**2.1.1.36**
COP9 signalosome complex subunit 4	0.75	0.06	8	285	24	46524.8	5.57	CSN4_HUMAN	COPS4	51138	n/a
Annexin A2*	**0.71**	**0.02**	**18**	**393**	**47**	**38807.9**	**7.57**	**ANXA2_HUMAN**	**ANXA2**	**302**	**n/a**
Heterogeneous nuclear ribonucleoproteins A2/B1*	**0.70**	**0.08**	**3**	**74**	**15**	**37463.8**	**8.97**	**ROA2_HUMAN**	**HNRNPA2B1**	**3181**	**n/a**
Triosephosphate isomerase*	**0.70**	**0.10**	**21**	**663**	**91**	**26937.8**	**6.45**	**TPIS_HUMAN**	**TPI1**	**7167**	**5.3.1.1**
Protein phosphatase methylesterase 1	0.68	0.09	6	87	21	42687.4	5.67	PPME1_HUMAN	PPME1	51400	3.1.1.-
Alpha-enolase*	**0.63**	**0.13**	**11**	**264**	**32**	**47481.4**	**7.01**	**ENOA_HUMAN**	**ENO1**	**2023**	**4.2.1.11**
Voltage-dependent anion-selective channel protein 2	0.60	0.12	5	131	31	38638.9	6.32	VDAC2_HUMAN	VDAC2	7417	n/a
Actin, cytoplasmic 2*	**0.56**	**0.11**	**9**	**315**	**28**	**42107.9**	**5.31**	**ACTG_HUMAN**	**ACTG1**	**71**	**n/a**
Actin, cytoplasmic 2*	**0.55**	**0.11**	**7**	**338**	**28**	**42107.9**	**5.31**	**ACTG_HUMAN**	**ACTG1**	**71**	**n/a**
Ribonuclease inhibitor	0.50	0.15	14	361	39	51765.8	4.71	RINI_HUMAN	RNH1	6050	n/a
Proteasome subunit beta type 6 precursor	0.49	0.17	3	74	13	25569.5	4.8	PSB6_HUMAN	PSMB6	5694	3.4.25.1
Actin, cytoplasmic 2*	**0.49**	**0.06**	**7**	**254**	**24**	**42107.9**	**5.31**	**ACTG_HUMAN**	**ACTG1**	**71**	**n/a**
Prefoldin subunit 5	0.44	0.05	2	95	10	17374	5.93	PFD5_HUMAN	PFDN5	5204	n/a
Malate dehydrogenase, cytoplasmic*	**0.40**	**0.18**	**4**	**88**	**19**	**36631.1**	**6.91**	**MDHC_HUMAN**	**MDH1**	**4190**	**1.1.1.37**
Ubiquitin-conjugating enzyme E2 N*	**0.34**	**0.17**	**8**	**369**	**38**	**17184**	**6.13**	**UBE2N_HUMAN**	**UBE2N**	**7334**	**6.3.2.19**
Protein DJ-1*	**0.31**	**0.07**	**2**	**112**	**7**	**20049.6**	**6.33**	**PARK7_HUMAN**	**PARK7**	**11315**	**n/a**
Inorganic pyrophosphatase	0.31	0.24	6	153	26	33095.3	5.54	IPYR_HUMAN	PPA1	5464	3.6.1.1

[a] Ratio: Fold-change of spot abundance of stressed cells vs control cells in the repeated exposure experiment. [b] SD: Standard deviation of the quantification data. [c] Number of peptides matching in the peptide mass fingerprint based identification. [d] Mascot Protein Score: obtained from the combined (MS and MS/MS data) database search. [e] Relative molecular mass of the protein as calculated from the amino acid sequence of the polypeptide without any co- or posttranslational modifications. [f] Calculated p*I* of the polypeptide as obtained from Swiss-Prot database. Proteins indicated by asterisks (bold rows) were found in significantly overrepresented biological processes following the PANTHER classification system.

the next neighbor approach resulted in additional 132 PIN derived candidates. The protein interaction network resting on this expanded list of 213 candidates was found as a large subgraph holding 195 protein nodes and 727 protein interactions. The remaining 18 candidates were found in one additional subgraph holding only 3 protein nodes, or did not provide interactions (Figure 4).

The procedure along next neighbor expansion is naturally prone to generation of larger subgraphs. For clarifying the relevance of the large subgraph identified by our procedure, we performed a reference computation of the mean number of protein nodes in the largest subgraphs derived on the basis of randomly picked protein lists of the same sample size as our expanded protein list ($n = 213$). This reference calculation

Table 3. Effects of Single and Repeated Exposure to PDF on Significantly Enriched Biological Processes in Immortalized Mesothelial Cells[a]

	single exposure						repeated exposure					
	100 candidates			next neighbor expansion			58 candidates			next neighbor expansion		
significantly enriched biological process	obs. no.[b]	exp. no.[c]	*p*-value	obs. no.	exp. no.	*p*-value	obs. no.	exp. no.	*p*-value	obs. no.	exp. no.	*p*-value
In Single and Repeated Exposure												
Cell structure and motility (1148)[d]	19	4.5	3.28×10^{-6}	33	10.6	2.61×10^{-7}	5	2.6		13	4.9	4.05×10^{-2}
Carbohydrate metabolism (592)	10	2.3	3.72×10^{-3}	14	5.5	4.11×10^{-2}	7	1.4	1.22×10^{-2}	8	2.5	1.27×10^{-1}
Immunity and defense (1318)	10	5.2		40	12.1	1.09×10^{-9}	6	3.0		18	5.7	3.99×10^{-4}
In Single Exposure												
Protein metabolism and modification (3040)	29	12.0	1.18×10^{-4}	76	28.0	3.97×10^{-15}	14	6.9		24	13.0	
Cell structure (687)	16	2.7	1.82×10^{-6}	24	6.3	4.72×10^{-6}	4	1.6		9	2.9	
Protein folding (186)	11	0.7	3.62×10^{-8}	21	1.7	2.02×10^{-14}	4	0.4		5	0.8	
Protein modification (1157)	9	4.6		38	10.7	1.78×10^{-9}	3	2.6		11	5.0	
Cell cycle (1009)	7	4.0		27	9.3	2.64×10^{-5}	4	2.3		11	4.3	
Protein complex assembly (68)	6	0.3	5.09×10^{-5}	9	0.6	2.93×10^{-6}	2	0.2		2	0.3	
Intracellular protein traffic (1008)	6	4.0		20	9.3	3.61×10^{-2}	5	2.3		6	4.3	
Stress response (200)	5	0.8		13	1.8	9.18×10^{-6}	3	0.5		3	0.9	
Signal transduction (3406)	5	13.4		60	31.3	1.30×10^{-5}	3	7.8		16	14.6	
Glycolysis (46)	5	0.2	1.83E-04	6	0.4	7.63×10^{-4}	2	0.1		2	0.2	
Cell cycle control (418)	2	1.6		15	3.9	1.43×10^{-3}	0	1.0		4	1.8	
In Repeated Exposure												
Nucleoside, nucleotide and nucleic acid metabolism (3343)	14	13.2		35	30.8		12	7.6		29	14.3	4.11×10^{-3}
Pre-mRNA processing (291)	6	1.1		8	2.7		5	0.7		7	1.3	4.01×10^{-2}
Apoptosis (531)	0	2.1		25	4.9		2	1.2		9	2.3	1.53×10^{-2}

[a] Given are the biological processes which show a significantly enriched population ($p < 0.05$, Bonferroni adjusted for multiple testing) following the PANTHER classification system with or without next neighbor expansion following single and repeated PDF exposure. [b] Obs. no.: observed number of genes for the Chi^2-test. [c] Exp. no.: expected number of genes for the Chi^2-test. [d] The numbers of NCBI genes assigned to the particular processes are given in parentheses. Nonsignificant *p*-values were omitted.

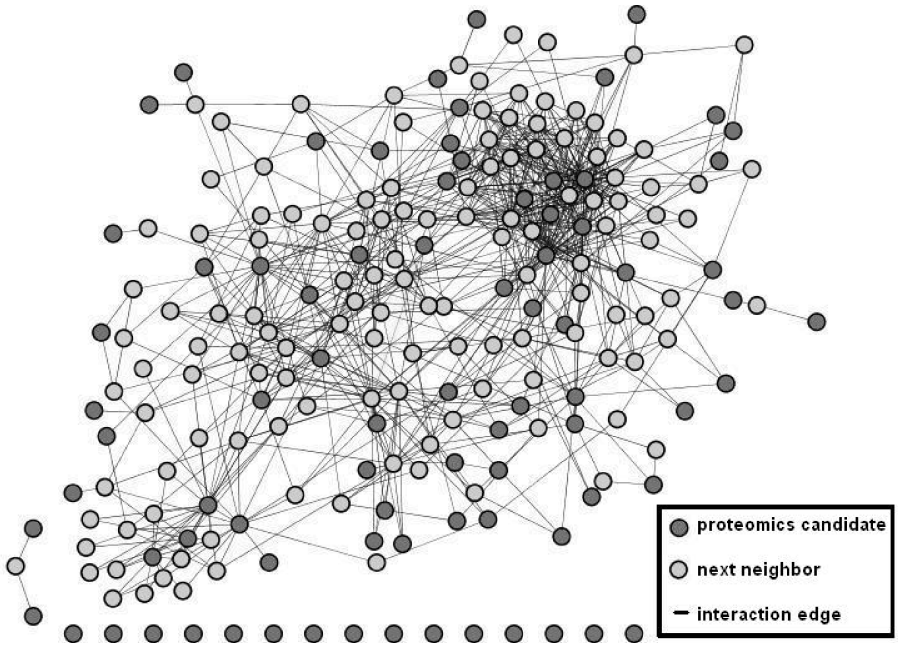

Figure 4. Representation of the PIN generated on the basis of the experimentally identified candidate list using OPHID interaction data. Proteomic candidates are represented by dark gray circles, next neighbors by light gray circles, and known interactions in the database are represented by lines connecting the circles representing the respective candidates. The graph shows the high interconnectivity of the largest subgraph (195 nodes), compared to the largest subgraphs found in the randomly picked data sets of the validation experiments (8 nodes on average).

showed on average only 8 nodes per largest subgraph (computed on the basis of 1000 randomized lists), clearly demonstrating the significance of the increased dependency between experimentally identified candidates in the next neighbor approach.

As second reference, we expanded randomly selected lists of 81 proteins each (corresponding to the number of proteins identified in the proteomics experiment and which were also found in the OPHID data set) by their respective next neighbors (1000 individual lists) to resemble the situation as given for the

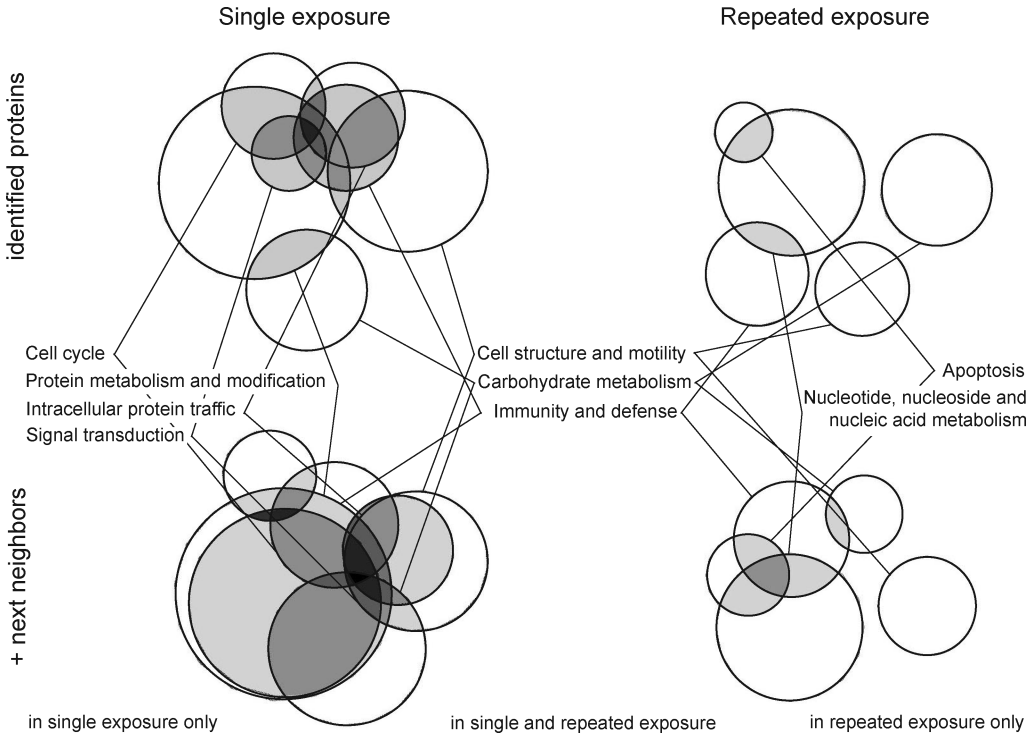

Figure 5. Venn diagrams showing the distribution of candidates with and without their next neighbors over the significantly enriched biological processes following single and repeated PDF exposure. Circles are indicated with the biological process they represent. Overlapping areas contain proteins which are present in multiple processes: the more processes overlap, the darker the area is presented. Processes solely containing proteins that are also in a significantly enriched parent process were omitted in the figure as described in Materials and Methods.

proteomics candidate list. This procedure intrinsically increased the mean number of protein nodes of the largest subgraph to about 90 protein nodes. However, the number of protein nodes of the largest subgraph derived on the basis of the expanded list of 81 candidates showed a significantly higher number of 195 protein nodes (Figure 4), also indicating an increased functional interplay of the 81 candidates initially identified in the proteomics experiment.

In the repeated exposure experiment, the PIN derived on the basis of the 58 identified candidates applying OPHID data resulted in a total graph of 47 protein nodes and 6 protein interaction edges. Eleven candidates were not listed in OPHID. The two equally largest subgraphs showed 3 protein candidates. Expanding the candidate list of 47 proteins also represented in OPHID by again utilizing the next neighbor approach resulted in additional 51 proteins. The PIN resting on this list of 98 proteins was found as a large subgraph holding 87 protein nodes and 209 protein interactions. The remaining 11 candidates did not provide interactions.

Analysis of Biological Processes after Next Neighbor Expansion. Recalculation of the significantly enriched biological processes using the expanded protein lists also including the experimentally identified proteins not listed in OPHID (232 proteins in the single exposure experiment and 109 proteins in the repeated exposure experiment) are also given in Table 3. All but one process in this table are overrepresented (comparing the observed vs expected number of process members). The only process which was found as significantly underrepresented following single and repeated PDF exposure, regardless of the inclusion of next neighbors, was 'biological process unclassified'. This process was omitted from the table as it represents a residual group of proteins not amenable to interpretation in the context of processes.

Interplay of Biological Processes. To compare the mesothelial stress responses to single and repeated PDF exposures, the conditioning effects observed after repeated PDF exposure were visualized using Venn diagrams showing the involvement of candidates in one or multiple biological processes (Figure 5). The diagrams for single exposure show more overlapping areas indicating a higher degree of multitasking proteins. Following single PDF exposure, 101 of 170 candidates in the expanded list (which also were members of significantly enriched biological processes) were involved in a single process, whereas 69 proteins were assigned to multiple biological processes. Following repeated PDF exposure, 56 of 65 candidates were involved in one, but only 9 in multiple biological processes. Repeated exposure resulted in involvement of 2.9-fold fewer "multi-tasking proteins" (Chi^2 $p = 9.8 \times 10^{-5}$, Pearson, two-sided). This phenomenon could be observed regardless of inclusion of the OPHID next neighbors which could, of course, affect the content of multitasking proteins by the inherent characteristics of the method (experimentally determined candidates only: Chi^2 $p = 4.2 \times 10^{-5}$, Pearson, two-sided).

This finding was validated in the subset of 45 candidates that showed an expression ratio of <0.9 or >1.1 in single exposure and could also be relocated in the repeated exposure experiment (Table 4). Consistent with the concept of conditioning, the probability of sustained activation following repeated PDF exposition was significantly less likely for multitasking proteins than for proteins involved in only one biological process (Chi^2 $p = 0.014$, Pearson, two-sided).

Discussion

Although some effects of PDF exposure have already been studied individually in experimental PD, the use of combined

Table 4. Attenuation of Cellular Responses Following Repeated PDF Exposure by Candidates Involved in Multiple Biological Processes[a]

Protein symbol	Protein metabolism and modification	Cell structure and motility	Carbohydrate metabolism	Intracellular protein traffic	Cell cycle	Immunity and defense	Signal transduction
PPIA	1			1		1	
ACTR1A		1		1	1		
ACTB		1		1	1		
RAN				1	1		1
HSPA8	1					1	
HSPA9	1					1	
HSPA1A	1					1	
TBCB	1	1					
UBE2V1	1				1		
UBE2A	1				1		
GANAB	1		1				
HADHA	1		1				
ANXA2		1		1			
GRB2						1	1
HSPD1	1						
HSPA4	1						
P4HB	1						
HCCS	1						
PDIA3	1						
TPM1		1					
GSN		1					
RDX		1					
MSN		1					
EZR		1					
CAPZA2		1					
KRT7		1					
LMNB1		1					
LMNA		1					
KRT8		1					
ALDOA			1				
PGAM1			1				
PKM2			1				
ENO1			1				
PCBP2	1						
TSFM	1						
SCRN1	1						
PSMD4	1						
SERPINH1	1						
PSMB3	1						
TALDO1			1				
IDH1			1				
NIPSNAP1				1			
C14orf166					1		
C1QBP						1	
STRAP							1

[a] Represented are 45 MS-identified proteins which were significantly altered following single exposure and could be relocated in the gels prepared from mesothelial cell lysates following repeated PDF exposure. The proteins were categorized by the significantly enriched biological processes (PANTHER) they were found to be involved in (columns) and by their expression pattern after repeated exposure. Rows which contain proteins that were no longer differentially abundant (effect of "classical conditioning") are shaded in dark gray.

proteomic and bioinformatic techniques enables an independent extension of a specific proteomic profile characterizing cellular responses and also specific interventions, such as conditioning. Our study, therefore, represents the first step toward global characterization of simultaneously elicited biological processes during recovery of mesothelial cells from single and repeated PDF exposure.

In good accordance with other cytotoxicity models, acute PDF exposure resulted in reduction of unspecific biological processes in favor of the cell's response to stress.[39] Evident was a massive activation of interwoven cellular responses that can be grouped into reparative mechanisms, including protein metabolism, modification and folding; cell structure modification; signaling; carbohydrate metabolism and inflammatory cellular processes.

Molecular chaperones, with HSP being the prototype, constituted a major subgroup of the identified proteins involved in these processes. HSP represent a large family of soluble proteins that are found throughout the mesothelial cell; the amount of all HSP isoforms in some instances can constitute up to 5% of total cellular proteins.[39] In previous studies in experimental PD, we have shown by Western blot analysis that the same insult that induces mesothelial cell injury also activates Hsp27 (HSPB1) and Hsp72 (HSPA1), the most abundant effectors of the cellular stress response.[11,12] These proteins are known to cooperate in transport and folding of proteins, without alteration of their own structure, by binding to hydrophobic, normally hidden domains of immature or denatured proteins. They may prevent aggregation or even resolubilize aggregated proteins. Interestingly, Hsp47 (SERPINH1) was also identified in our present study. This collagen specific chaperone is involved in PDF induced peritoneal fibrosis and may be affected by the antifibrotic drug pirfenidone.[40,41] It is thus likely that several HSP might be attractive therapeutic target proteins in PD.

In addition, our study identified additional chaperones (HSPA4, Hsp60 (HSPD1), Grp75 (HSPA9, mortalin), Grp94 (HSP90B1), P4HB, PDIA3, PPIA (cyclophilin A), TBCB, CCT2, CCT7) that have not yet been described in PD. Several of these novel players are ER stress proteins (e.g., Hsp47, Hsp60, Grp75, Grp94) and, as in some cases suggested by their name ("glucose-regulated-protein"), expected to be regulated by glucose based PDF.[12,14] Involvement of the ubiquitin proteasome pathway, represented by PSMA2, PSMB3, PSMD4, UBE2V1 and UBE2A, confirms the relevance of the cellular protein repair and degradation machinery for mesothelial cell outcome in PD.

Cytoskeletal proteins identified in enriched biological processes were actin (ACTA1, ACTB), cytokeratine (KRT7, KRT8), tropomyosine (TPM1, TPM2), myosine (MLRM, MLRN) and members of the ERM family (EZR, RDX, MSN) which contribute to the epithelial appearance and function of mesothelial cells by linking actin to the plasma membrane and enabling microvilli biogenesis.[42] The involvement of these proteins confirms cytoskeletal damage, epithelial to mesenchymal transdifferentiation (EMT) and cellular remodeling as important mechanisms mediating PDF induced mesothelial cell injury.[13,43–46] Several proteins with strong affinity to cytoskeletal proteins are also involved in pathways like 'protein modification', 'protein folding' or 'protein complex assembly'. Other proteins in the data set with strong cytoskeletal association are actin capping proteins (CAPZA2, CAPG), gelsolin (GSN), twinfilin-2 (TWF2), T-complex proteins (CCT2, CCT7) which regulate actin polymerization, and TBCB which is a cofactor for tubulin folding. The already mentioned Hsp47 and PLOD3 both stabilize collagens and procollagens. 14-3-3ε (YWHAE) regulates actin polymerization via interaction with Hsp27 and is also a

member of the significantly enriched processes 'cell cycle' and 'signal transduction', interacting with HSF1.[47] Finally, annexin 2 (ANXA2) plays a role in cytoskeletal development but is also part of the protein kinase C (PKC) signaling and Ras pathways, demonstrating the close interactions between these stress-induced cellular processes in experimental PD.

Another functionally interwoven set of proteins can be assigned to immunity and defense processes. Peritoneal mesothelial cells are known to produce cytokines like IL-1β, IL-6, IL-8 and TNF-α and to overexpress adhesion molecules when stimulated.[48–50] Besides the group of molecular chaperones, our data revealed involvement of novel players like cyclophilin A (PPIA), peroxiredoxin (PRDX1) and growth factor receptor-bound protein 2 (GRB2). PPIA not only shows activity in protein folding as a peptidylprolyl *cis*−*trans*-isomerase,[51] but is also a member of the immunophilin family[52] and the receptor for the immunosuppressive drugs tacrolimus and cyclosporine.[53,54] Peroxiredoxin is induced by TGF-beta and influences NF-κB activity,[55,56] whereas GRB2 is a member of the Ras signaling pathway.[57] We also found a member of the nuclear analogon of this pathway by identification of the GTPase RAN. Another GTPase signaling mechanism is represented by the G protein GNB2L1 (RACK1) which is the receptor of activated protein kinase C (PKC). RACK1 is therefore also a member of the significantly enriched biological process 'signal transduction' and regulates HIF1 by dimerization and competition with Grp94. RACK1 is known to modulate STAT1 and TYK2 and activates JNK via PKC, thus, representing a link to the stress kinase pathways.[58]

Taken together, acute PDF exposure activates molecular pathways that involve a significant number of proteins being players in more than one cellular process. Whereas the majority of these processes contribute to protection of cells under acute stressful conditions, some of them may be deleterious for the peritoneal membrane in response to chronic PDF exposure.[48–50] Data like ours might allow identifying novel candidates as biomarkers.

In the second part of this study, we compared the cellular responses following single versus repeated PDF exposure. In the clinical setting, PD consists of repeated exposure of mesothelial cells to PDF, and complex intracellular cross-talk will likely decide the mesothelial cell's fate after recurring stressful stimuli. One particularly well-described example for such cross-talk is "classic conditioning". In classic conditioning, the pretreatment of a cell with a given stressor modulates the responses of this cell against repeated treatment with the same stressor. These effects are almost exclusively regulated at the protein level, based on protein−protein interactions.[59,60] PDF pretreatment of mesothelial cells has previously been shown to induce cytoprotection and enhanced cytoskeletal repair, mediated by molecular chaperones.[15] In this study, we searched for more global effects of the PDF pretreatment. Obviously, proteomic analysis is a particularly attractive tool to assess the cellular effects of such an intervention.

In our study, cellular reaction to the repeated stress was indeed attenuated by prior pretreatment, resulting in activation of a lower number of biological processes. Only few candidates from single exposure could be reidentified; a majority of identified proteins were new players. Besides carbohydrate metabolism, the processes related to cell structure, immunity and defense remained consistently activated. Nearly all processes related to protein metabolism and modification, including chaperoning and stress response, failed to reach significant levels after the second PDF treatment. Interestingly, nucleic acid processing and apoptosis became significantly enriched (with new players such as PCNA also known as cyclin), reflecting a reactive increase in mesothelial cell turnover as previously described in the *in vivo* setting.[61] In direct comparison at the protein level, the majority of multitasking proteins, most of them involved in protein metabolism and modification, lost their differential expression following repeated PDF exposure. Besides these chaperons, the small GTPase RAN and the adaptor protein GRB2 also returned to control levels following repeated PDF exposure. Interestingly, these proteins are members of the ras signaling pathway, and inhibition of that pathway during acute stress represented a major mechanism in other models of conditioning.[62] Taken together, the second PDF exposure resulted in changes of the protein profile that were less attributable to acute cellular injury responses.

Overall, repeated PDF exposure resulted in a less interwoven distribution of activated cellular processes than single exposure, consistent with a reduced number of involved multitasking proteins. This finding agrees well with expected conditioning effects and cytoprotection: Upon acute exposure to a stress, at a time when the "protein machinery" is not optimized, mesothelial cells respond by activating a common stress response that results in differential expression of multitasking proteins. These proteins are likely involved in multiple biological processes in order to protect against a wide range of cellular stressors. Upon repeated exposure to the same stressor, at a time when the cellular levels of molecular chaperones are increased, mesothelial cells respond with attenuated stress response, as most of the stress-induced proteins are regulated in a negative feedback loop. Members of the molecular chaperones are particularly well-known as suppressors for stress-activated stress kinases and transcription factors.[63–65] The observed protein expression pattern is therefore congruent with the concept of conditioning effects. Additionally, repetitive exposure to the same stressor will likely result in reduced common cellular stress responses but rather increase adaption to the new condition, resulting in involvement of more specific proteins. Such cellular adaption has been previously demonstrated in renal tubular cells exposed to acute versus chronic hyperosmolar stress.[66]

In summary, this study describes elements of the reprogrammed proteome of human mesothelial cells during recovery from exposure to cytotoxic properties of PDF. Interestingly, repeated exposure results in a markedly different pattern of cellular responses that are at least in part consistent with the concept of conditioning effects. More detailed comparison of the mesothelial cell proteome changes, using long-term experiments with more repeated PDF exposures, will likely allow us to search for specific adaptive changes and to identify additional candidates for interventions based on manipulation of the cellular stress responses. Certainly, future experiments in the *in vivo* model are needed to prove the biological relevance of these findings.[67,68]

Acknowledgment. The presented work was funded by the FWF (Austrian Science Fund) Project P18130−B13 (to C.A.).

Supporting Information Available: A representative MS/MS spectrum and Supplemental material to Tables 1 and 2 giving details of the MS and MS/MS protein identification results are included in the Supporting Information. This

material is available free of charge via the Internet at http://pubs.acs.org.

References

(1) Davies, S. J.; Phillips, L.; Griffiths, A. M.; Russell, L. H.; Naish, P. F.; Russell, G. I. What really happens to people on long-term peritoneal dialysis. *Kidney Int.* **1998**, *54* (6), 2207–17.

(2) Topley, N. What is the ideal technique for testing the biocompatibility of peritoneal dialysis solutions. *Peritoneal Dial. Int.* **1995**, *15* (6), 205–9.

(3) Breborowicz, A.; Oreopoulos, D. G. Biocompatibility of peritoneal dialysis solutions. *Am. J. Kidney Dis.* **1996**, *27* (5), 738–43.

(4) Catalan, M. P.; Reyero, A.; Egido, J.; Ortiz, A. Acceleration of neutrophil apoptosis by glucose-containing peritoneal dialysis solutions: role of caspases. *J. Am. Soc. Nephrol.* **2001**, *12* (11), 2442–9.

(5) Cendoroglo, M.; Sundaram, S.; Groves, C.; Ucci, A. A.; Jaber, B. L.; Pereira, B. J. Necrosis and apoptosis of polymorphonuclear cells exposed to peritoneal dialysis fluids in vitro. *Kidney Int.* **1997**, *52* (6), 1626–34.

(6) Jorres, A.; Topley, N.; Gahl, G. M. Biocompatibility of peritoneal dialysis fluids. *Int. J. Artif. Organs* **1992**, *15* (2), 79–83.

(7) Plum, J.; Lordnejad, M. R.; Grabensee, B. Effect of alternative peritoneal dialysis solutions on cell viability, apoptosis/necrosis and cytokine expression in human monocytes. *Kidney Int.* **1998**, *54* (1), 224–35.

(8) Plum, J.; Razeghi, P.; Lordnejad, R. M.; Perniok, A.; Fleisch, M.; Fussholler, A.; Schneider, M.; Grabensee, B. Peritoneal dialysis fluids with a physiologic pH based on either lactate or bicarbonate buffer-effects on human mesothelial cells. *Am. J. Kidney Dis.* **2001**, *38* (4), 867–75.

(9) Witowski, J.; Topley, N.; Jorres, A.; Liberek, T.; Coles, G. A.; Williams, J. D. Effect of lactate-buffered peritoneal dialysis fluids on human peritoneal mesothelial cell interleukin-6 and prostaglandin synthesis. *Kidney Int.* **1995**, *47* (1), 282–93.

(10) Yang, A. H.; Chen, J. Y.; Lin, Y. P.; Huang, T. P.; Wu, C. W. Peritoneal dialysis solution induces apoptosis of mesothelial cells. *Kidney Int.* **1997**, *51* (4), 1280–8.

(11) Arbeiter, K.; Bidmon, B.; Endemann, M.; Bender, T. O.; Eickelberg, O.; Ruffingshofer, D.; Mueller, T.; Regele, H.; Herkner, K.; Aufricht, C. Peritoneal dialysate fluid composition determines heat shock protein expression patterns in human mesothelial cells. *Kidney Int.* **2001**, *60* (5), 1930–7.

(12) Aufricht, C.; Endemann, M.; Bidmon, B.; Arbeiter, K.; Mueller, T.; Regele, H.; Herkner, K.; Eickelberg, O. Peritoneal dialysis fluids induce the stress response in human mesothelial cells. *Peritoneal Dial. Int.* **2001**, *21* (1), 85–8.

(13) Endemann, M.; Bergmeister, H.; Bidmon, B.; Boehm, M.; Csaicsich, D.; Malaga-Dieguez, L.; Arbeiter, K.; Regele, H.; Herkner, K.; Aufricht, C. Evidence for HSP-mediated cytoskeletal stabilization in mesothelial cells during acute experimental peritoneal dialysis. *Am. J. Physiol.: Renal Physiol.* **2007**, *292* (1), F47–56.

(14) Aufricht, C. HSP: helper, suppressor, protector. *Kidney Int.* **2004**, *65* (2), 739–40.

(15) Bidmon, B.; Endemann, M.; Arbeiter, K.; Ruffingshofer, D.; Regele, H.; Herkner, K.; Eickelberg, O.; Aufricht, C. Overexpression of HSP-72 confers cytoprotection in experimental peritoneal dialysis. *Kidney Int.* **2004**, *66* (6), 2300–7.

(16) Aufricht, C.; Bidmon, B.; Ruffingshofer, D.; Regele, H.; Herkner, K.; Siegel, N. J.; Kashgarian, M.; Van Why, S. K. Ischemic conditioning prevents Na, K-ATPase dissociation from the cytoskeletal cellular fraction after repeat renal ischemia in rats. *Pediatr. Res.* **2002**, *51* (6), 722–7.

(17) Gray, C. C.; Amrani, M.; Yacoub, M. H. Heat stress proteins and myocardial protection: experimental model or potential clinical tool. *Int. J. Biochem. Cell Biol.* **1999**, *31* (5), 559–73.

(18) Kabakov, A. E.; Budagova, K. R.; Latchman, D. S.; Kampinga, H. H. Stressful preconditioning and HSP70 overexpression attenuate proteotoxicity of cellular ATP depletion. *Am. J. Physiol.: Cell Physiol.* **2002**, *283* (2), C521–34.

(19) Beck, F. X.; Grunbein, R.; Lugmayr, K.; Neuhofer, W. Heat shock proteins and the cellular response to osmotic stress. *Cell Physiol. Biochem.* **2000**, *10* (5−6), 303–6.

(20) Neuhofer, W.; Lugmayr, K.; Fraek, M. L.; Beck, F. X. Regulated overexpression of heat shock protein 72 protects Madin-Darby canine kidney cells from the detrimental effects of high urea concentrations. *J. Am. Soc. Nephrol.* **2001**, *12* (12), 2565–71.

(21) Neuhofer, W.; Muller, E.; Burger-Kentischer, A.; Fraek, M. L.; Thurau, K.; Beck, F. Pretreatment with hypertonic NaCl protects MDCK cells against high urea concentrations. *Pfluegers Arch.* **1998**, *435* (3), 407–14.

(22) Santos, B. C.; Chevaile, A.; Hebert, M. J.; Zagajeski, J.; Gullans, S. R. A combination of NaCl and urea enhances survival of IMCD cells to hyperosmolality. *Am. J. Physiol.* **1998**, *274* (6 Pt. 2), F1167–73.

(23) Sheikh-Hamad, D.; Garcia-Perez, A.; Ferraris, J. D.; Peters, E. M.; Burg, M. B. Induction of gene expression by heat shock versus osmotic stress. *Am. J. Physiol.* **1994**, *267* (1 Pt. 2), F28–34.

(24) Crosby, L. M.; Hyder, K. S.; DeAngelo, A. B.; Kepler, T. B.; Gaskill, B.; Benavides, G. R.; Yoon, L.; Morgan, K. T. Morphologic analysis correlates with gene expression changes in cultured F344 rat mesothelial cells. *Toxicol. Appl. Pharmacol.* **2000**, *169* (3), 205–21.

(25) Sinha, P.; Poland, J.; Schnolzer, M.; Celis, J. E.; Lage, H. Characterization of the differential protein expression associated with thermoresistance in human gastric carcinoma cell lines. *Electrophoresis* **2001**, *22* (14), 2990–3000.

(26) Gorg, A.; Weiss, W.; Dunn, M. J. Current two-dimensional electrophoresis technology for proteomics. *Proteomics* **2004**, *4* (12), 3665–85.

(27) Knepper, M. A. Proteomics and the kidney. *J. Am. Soc. Nephrol.* **2002**, *13* (5), 1398–408.

(28) Thongboonkerd, V. Proteomics in nephrology: current status and future directions. *Am. J. Nephrol.* **2004**, *24* (3), 360–78.

(29) Perco, P.; Pleban, C.; Kainz, A.; Lukas, A.; Mayer, B.; Oberbauer, R. Gene expression and biomarkers in renal transplant ischemia reperfusion injury. *Transplant Int.* **2007**, *20* (1), 2–11.

(30) Perco, P.; Pleban, C.; Kainz, A.; Lukas, A.; Mayer, G.; Mayer, B.; Oberbauer, R. Protein biomarkers associated with acute renal failure and chronic kidney disease. *Eur. J. Clin. Invest.* **2006**, *36* (11), 753–63.

(31) Wessel, D.; Flugge, U. I. A method for the quantitative recovery of protein in dilute solution in the presence of detergents and lipids. *Anal. Biochem.* **1984**, *138* (1), 141–3.

(32) Shevchenko, A.; Wilm, M.; Vorm, O.; Mann, M. Mass spectrometric sequencing of proteins silver-stained polyacrylamide gels. *Anal. Chem.* **1996**, *68* (5), 850–8.

(33) Alter, O.; Brown, P. O.; Botstein, D. Singular value decomposition for genome-wide expression data processing and modeling. *Proc. Natl. Acad. Sci. U.S.A.* **2000**, *97* (18), 10101–6.

(34) Perco, P.; Rapberger, R.; Siehs, C.; Lukas, A.; Oberbauer, R.; Mayer, G.; Mayer, B. Transforming omics data into context: bioinformatics on genomics and proteomics raw data. *Electrophoresis* **2006**, *27* (13), 2659–75.

(35) Brown, K. R.; Jurisica, I. Online predicted human interaction database. *Bioinformatics* **2005**, *21* (9), 2076–82.

(36) Chen, J. Y.; Shen, C.; Sivachenko, A. Y. Mining Alzheimer disease relevant proteins from integrated protein interactome data. *Pac. Symp. Biocomput.* **2006**, 367–78.

(37) Platzer, A.; Perco, P.; Lukas, A.; Mayer, B. Characterization of protein-interaction networks in tumors. *BMC Bioinf.* **2007**, *8*, 224.

(38) Mi, H.; Guo, N.; Kejariwal, A.; Thomas, P. D. PANTHER version 6: protein sequence and function evolution data with expanded representation of biological pathways. *Nucleic Acids Res.* **2007**, *35*, D247–52.

(39) Morimoto, R. I. *The Biology of Heat Shock Proteins and Molecular Chaperones*; Cold Spring Harbor Laboratory Press: Plainview, NY, 1994; Vol. 26, pp 1−594.

(40) Mishima, Y.; Miyazaki, M.; Abe, K.; Ozono, Y.; Shioshita, K.; Xia, Z.; Harada, T.; Taguchi, T.; Koji, T.; Kohno, S. Enhanced expression of heat shock protein 47 in rat model of peritoneal fibrosis. *Peritoneal Dial. Int.* **2003**, *23* (1), 14–22.

(41) Nakayama, S.; Mukae, H.; Sakamoto, N.; Kakugawa, T.; Yoshioka, S.; Soda, H.; Oku, H.; Urata, Y.; Kondo, T.; Kubota, H.; Nagata, K.; Kohno, S. Pirfenidone inhibits the expression of HSP47 in TGF-beta1-stimulated human lung fibroblasts. *Life Sci.* **2008**, *82* (3−4), 210–7.

(42) Hughes, S. C.; Fehon, R. G. Understanding ERM proteins—the awesome power of genetics finally brought to bear. *Curr. Opin. Cell Biol.* **2007**, *19* (1), 51–6.

(43) Yung, S.; Davies, M. Response of the human peritoneal mesothelial cell to injury: an in vitro model of peritoneal wound healing. *Kidney Int.* **1998**, *54* (6), 2160–9.

(44) Selgas, R.; Fernandez de Castro, M.; Viguer, J. M.; Burgos, E.; Bajo, M. A.; Carcamo, C.; Vara, F. Transformed mesothelial cells in patients on CAPD for medium- to long-term periods. *Peritoneal Dial. Int.* **1995**, *15* (8), 305–11.

(45) Vargha, R.; Endemann, M.; Kratochwill, K.; Riesenhuber, A.; Wick, N.; Krachler, A. M.; Malaga-Dieguez, L.; Aufricht, C.; Ex vivo reversal of in vivo transdifferentiation in mesothelial cells grown from peritoneal dialysate effluents. *Nephrol., Dial., Transplant.* **2006**.

(46) Vargha, R.; Bender, T. O.; Riesenhuber, A.; Endemann, M.; Kratochwill, K.; Aufricht, C. Effects of epithelial-to-mesenchymal transition on acute stress response in human peritoneal mesothelial cells. *Nephrol., Dial., Transplant.* **2008**, *23* (11), 3494–500.
(47) Wang, X.; Grammatikakis, N.; Siganou, A.; Stevenson, M. A.; Calderwood, S. K. Interactions between extracellular signal-regulated protein kinase 1, 14-3-3epsilon, and heat shock factor 1 during stress. *J. Biol. Chem.* **2004**, *279* (47), 49460–9.
(48) Bender, T. O.; Riesenhuber, A.; Endemann, M.; Herkner, K.; Witowski, J.; Jorres, A.; Aufricht, C. Correlation between HSP-72 expression and IL-8 secretion in human mesothelial cells. *Int. J. Artif. Organs* **2007**, *30* (3), 199–203.
(49) Jorres, A.; Ludat, K.; Lang, J.; Sander, K.; Gahl, G. M.; Frei, U.; DeJonge, K.; Williams, J. D.; Topley, N. Establishment and functional characterization of human peritoneal fibroblasts in culture: regulation of interleukin-6 production by proinflammatory cytokines. *J. Am. Soc. Nephrol.* **1996**, *7* (10), 2192–201.
(50) Topley, N.; Jorres, A.; Luttmann, W.; Petersen, M. M.; Lang, M. J.; Thierauch, K. H.; Muller, C.; Coles, G. A.; Davies, M.; Williams, J. D. Human peritoneal mesothelial cells synthesize interleukin-6: induction by IL-1 beta and TNF alpha. *Kidney Int.* **1993**, *43* (1), 226–33.
(51) Kofron, J. L.; Kuzmic, P.; Kishore, V.; Colon-Bonilla, E.; Rich, D. H. Determination of kinetic constants for peptidyl prolyl cis-trans isomerases by an improved spectrophotometric assay. *Biochemistry* **1991**, *30* (25), 6127–34.
(52) Galat, A. Peptidylproline cis-trans-isomerases: immunophilins. *Eur. J. Biochem.* **1993**, *216* (3), 689–707.
(53) Fruman, D. A.; Mather, P. E.; Burakoff, S. J.; Bierer, B. E. Correlation of calcineurin phosphatase activity and programmed cell death in murine T cell hybridomas. *Eur. J. Immunol.* **1992**, *22* (10), 2513–7.
(54) Liu, J.; Farmer, J. D., Jr.; Lane, W. S.; Friedman, J.; Weissman, I.; Schreiber, S. L. Calcineurin is a common target of cyclophilin-cyclosporin A and FKBP-FK506 complexes. *Cell* **1991**, *66* (4), 807–15.
(55) Jin, D. Y.; Chae, H. Z.; Rhee, S. G.; Jeang, K. T. Regulatory role for a novel human thioredoxin peroxidase in NF-kappaB activation. *J. Biol. Chem.* **1997**, *272* (49), 30952–61.
(56) Yun, S. J.; Seo, J. J.; Chae, J. Y.; Lee, S. C. Peroxiredoxin I and II are up-regulated during differentiation of epidermal keratinocytes. *Arch. Dermatol. Res.* **2005**, *296* (12), 555–9.
(57) Takenawa, T.; Miki, H.; Matuoka, K. Signaling through Grb2/Ash-control of the Ras pathway and cytoskeleton. *Curr. Top. Microbiol. Immunol.* **1998**, *228*, 325–42.
(58) Lopez-Bergami, P.; Habelhah, H.; Bhoumik, A.; Zhang, W.; Wang, L. H.; Ronai, Z. RACK1 mediates activation of JNK by protein kinase C [corrected]. *Mol. Cell* **2005**, *19* (3), 309–20.
(59) Beere, H. M.; Wolf, B. B.; Cain, K.; Mosser, D. D.; Mahboubi, A.; Kuwana, T.; Tailor, P.; Morimoto, R. I.; Cohen, G. M.; Green, D. R. Heat-shock protein 70 inhibits apoptosis by preventing recruitment of procaspase-9 to the Apaf-1 apoptosome. *Nat. Cell Biol.* **2000**, *2* (8), 469–75.
(60) Jaattela, M. Heat shock proteins as cellular lifeguards. *Ann. Med.* **1999**, *31* (4), 261–71.
(61) Gotloib, L.; Shostak, A.; Wajsbrot, V.; Kushnier, R. High glucose induces a hypertrophic, senescent mesothelial cell phenotype after long in vivo exposure. *Nephron* **1999**, *82* (2), 164–73.
(62) Benter, I. F.; Juggi, J. S.; Khan, I.; Yousif, M. H.; Canatan, H.; Akhtar, S. Signal transduction mechanisms involved in cardiac preconditioning: role of Ras-GTPase, Ca2+/calmodulin-dependent protein kinase II and epidermal growth factor receptor. *Mol. Cell. Biochem.* **2005**, *268* (1−2), 175–83.
(63) Morimoto, R. I. Regulation of the heat shock transcriptional response: cross talk between a family of heat shock factors, molecular chaperones, and negative regulators. *Genes Dev.* **1998**, *12* (24), 3788–96.
(64) Morimoto, R. I.; Kline, M. P.; Bimston, D. N.; Cotto, J. J. The heat-shock response: regulation and function of heat-shock proteins and molecular chaperones. *Essays Biochem.* **1997**, *32*, 17–29.
(65) Pirkkala, L.; Alastalo, T. P.; Zuo, X.; Benjamin, I. J.; Sistonen, L. Disruption of heat shock factor 1 reveals an essential role in the ubiquitin proteolytic pathway. *Mol. Cell. Biol.* **2000**, *20* (8), 2670–5.
(66) Beck, F. X.; Neuhofer, W.; Muller, E. Molecular chaperones in the kidney: distribution, putative roles, and regulation. *Am. J. Physiol.: Renal Physiol.* **2000**, *279* (2), F203–15.
(67) Lameire, N.; Van Biesen, W.; Van Landschoot, M.; Wang, T.; Heimburger, O.; Bergstrom, J.; Lindholm, B.; Hekking, L. P.; Havenith, C. E.; Beelen, R. H. Experimental models in peritoneal dialysis: a European experience. *Kidney Int.* **1998**, *54* (6), 2194–206.
(68) ter Wee, P. M.; Beelen, R. H.; van den Born, J. The application of animal models to study the biocompatibility of bicarbonate-buffered peritoneal dialysis solutions. *Kidney Int. Suppl.* **2003**, (88), S75–83.

PR800916S